

1 **BASELINE CHARACTERIZATION OF ENVIRONMENTAL**
2 **CONDITIONS LEADING UP TO MARINE PROTECTED**
3 **AREA ESTABLISHMENT IN THE NORTH-CENTRAL COAST**
4 **STUDY REGION**

5
6
7
8
9 William J. Sydeman^{1,2}, Sarah Ann Thompson^{1,3}, Marisol Garcia-Reyes¹,
10 and Mati Kahru²

11
12 ¹Farallon Institute for Advanced Ecosystem Research
13 Petaluma, CA 94952
14 www.faralloninstitute.org
15 www.faralloninstitute2.wordpress.com

16
17 ²Integrative Oceanography, Scripps Institution of Oceanography
18 La Jolla, CA 95060

19
20 ³Climate Impacts Group, University of Washington, Seattle, WA 98115
21
22
23



Revised Final Report: 1 October 2013

This page intentionally left blank.

Table of Contents

33		
34		
35	Assessment of Project Goals and Accomplishments	5
36	Executive Summary	7
37	Revised Final Report.....	9
38	1. Introduction	10
39	2. Methods	11
40	2.1. Data.....	12
41	2.1.1. Indicators of Transport from the Tropics.....	12
42	2.1.2. Indicators of Transport from the Extra-Tropics	12
43	2.1.3. Indicators of Regional Upwelling	13
44	2.1.4. Indicators of Local Current Flows.....	13
45	2.1.5. Indicators of Local Atmospheric and Hydrographic Conditions	14
46	2.1.6. Lower Trophic Level Indicator	14
47	2.1.7. Upper Trophic Level Indicator	15
48	2.2. Data Processing and Statistical Analyses	15
49	3. Results.....	16
50	3.1. Status and Trends in Basin-Scale Indicators.....	16
51	3.2. Status and Trends in Regional Upwelling Indicators	16
52	3.3. Status and Trends in Regional and Local-Scale Current Indicators	16
53	3.4. Status and Trends in Regional Wind and Hydrographic Indicators.....	17
54	3.5. Status and Trends in Regional Air Temperature and Precipitation Indicators	
55	17
56	3.6. Variable-Specific Multivariate Indicators.....	17
57	3.7. Correlations Among Physical Environmental Indicators	17
58	3.8. Development of Seasonal Multivariate Ocean-Climate Indicators (MOCI)	
59	18
60	3.9. Trends in MOCI	18
61	3.10. Correlations between MOCI, Large-Scale Climate Indices, and Local	
62	Measurements	19
63	3.11. Status and Trends of Biological Indicators.....	19
64	3.12. Correlations between Environmental and Biological Indicators	19
65	4. Discussion	19
66	4.1. Indicator Design and Development.....	19
67	4.2. Trends in Environmental Conditions.....	20
68	4.3. Relationships between Indicators	21
69	4.4. Environmental Conditions Immediately Preceding MPA Establishment	21
70	4.5. Linking Environmental and Biological Indicators.....	22
71	5. Conclusion	22
72	6. Acknowledgments.....	23
73	7. Literature Cited	24
74		

Tables and Figures

75		
76		
77		
78	Table 1. Data sets used.	29
79	Table 2. Trends based on Spearman rank correlation for physical variables, 1990-2010.	
80	31
81	Table 3. Results of principal components analysis within variable types, 1990-2010.	
82	33
83	Table 4. Interrelationships between environmental indicators.	35
84	Table 5. Seasonal multivariate ocean-climate indicators (MOCI) derived by principal	
85	component analysis (PCA).	37
86	Table 6. Cross-correlation of seasonal MOCI produced by principal component analysis	
87	(PCA), local variables only combined with PCA, and climate indices only combined with	
88	PCA.	38
89	Table 7. Spearman rank correlations of seabird reproductive success residuals and	
90	PC1 _{seabirds} and seasonal MOCI.	39
91		
92		
93	Figure 1. Indicators of El Niño/La Niña, transport from the tropics.	40
94	Figure 2. Indicators of transport from the sub-arctic North Pacific.	41
95	Figure 3. A. Indicators of regional upwelling.	42
96	Figure 4. Indicators of large-scale and local current flow.	43
97	Figure 5. Indicators of regional coupled wind and hydrography (1990-2010).	44
98	Figure 6. Indicators of regional atmospheric conditions.	45
99	Figure 7. The first principal component variable loadings plotted against the second	
100	principal component variable loadings (PC space), 1990-2010 for seasonal MOCI.	
101	46
102	Figure 8. Seasonal MOCI against time.	47
103	Figure 9. Seasonal MOCI time series, 1990-2010.	48
104	Figure 10. A. Log chlorophyll-a abundance anomalies (1997-2011).	49
105	Figure 11. Significant relationships for spring MOCI (PC1) and residuals of reproductive	
106	success for seabirds.	50
107		
108		
109		

110 A. Assessment of Project Goals and Accomplishments

111

112 Recognizing past and ongoing change in environmental conditions (climatological,
113 oceanographic, and ecological), the Monitoring Enterprise requested an assessment of
114 environmental conditions leading up to MPA implementation in the NCC region. This
115 work was designed to promote a better understanding of baseline monitoring results.
116 As many if not most biological populations in the region respond to environmental
117 variation, evaluating coupled climate-ecosystem variability is essential to detect and
118 subsequently attribute changes in MPAs to management actions. In this project, we
119 addressed this specific need for the NCC MPA biological monitoring program.

120

121 Fundamentally, our project was a task of integration. To accomplish this project, we
122 proposed to develop and report upon a suite of integrated *multivariate indicators* of (a)
123 “ocean climate”, and (b) biological populations and productivity, which together may
124 serve to characterize the state of the regional ecosystem.

125

126 Using our *Integrated Marine Ecological Database (IMED)*; Farallon Inst., unpubl.), we
127 focused on developing *multivariate ocean climate indicators* (hereafter *MOCI*). *MOCI*
128 were based on a compilation of 16 well-known large-scale to regional indicators (details
129 provided in our final report). As proposed, we compiled data for each season from
130 1990-2010, and produced seasonal *MOCI* using Principal Component/Empirical
131 Orthogonal Function analysis. As proposed, we were able to test the relationships
132 between *MOCI* and lower and upper trophic level ecosystem components including a
133 measurement of phytoplankton biomass (chl-a concentration – a combined product from
134 OCTS, SeaWiFS, and MODIS) and seabird productivity (breeding success of 4 species
135 from the Farallon Islands).

136

137 As proposed, we analyzed each of the indicator data sets for trends in “state” (mean)
138 and “variability” (variance). In comparison with other environmental syntheses, this
139 analysis is significant in that (a) it focuses on the NNC region (previous work has been
140 on the scale of the entire California Current), (b) it includes indicators that have yet to be
141 integrated in other ecosystem status reports (e.g., surface currents from the State of
142 California’s HF radar array), and (c) the *MOCI* are intuitive and interpretable and as
143 such should be accessible to the MPA management community (Monitoring Enterprise,
144 CDFW).

145

146 We also proposed to augment **IMED** with new data collected during the baseline
147 monitoring efforts, but unfortunately were not able to integrate these data because the
148 data are not yet available from other project PIs. We could have foreseen this issue
149 with the timing of availability of new NCC MPA monitoring data, but during the proposal
150 process, this did not occur to us, the ME, or other project PIs.

151

152 Overall, we accomplished most project goals and are satisfied with project results
153 (statistical integration of environmental indicators). This information should be of
154 considerable value to the State of California for understanding and evaluating results of

155 baseline MPA monitoring in the NCC region. We have also submitted a paper based on
156 this project for publication in the journal *Progress in Oceanography*.
157
158

159 **B. Executive Summary – Integrated Ecosystem Assessment (Sydeman and**
160 **Thompson, Revised 1 October 2013)**
161

- 162 1. California’s nearshore marine life is responsive to year-to-year and longer-term
163 changes in ocean conditions. In particular, growth/size, production, and
164 abundance of fish and other taxa are known to change with variation in water
165 temperature, upwelling-favorable winds, and currents. Therefore, baseline
166 information on variability in ocean conditions is required to understand and
167 evaluate changes in populations in this region. This context is critical to
168 monitoring population change and adaptive management of Marine Protected
169 Areas (MPA) in California. Without a simultaneous assessment of the effects of
170 ocean conditions, it will be difficult to formally attribute changes in populations to
171 the protection afforded by MPA designations.
172
- 173 2. In this report, we develop and explore comprehensive indicators of temporal
174 variability in ocean conditions over a 21-year period preceding the establishment
175 of MPAs along California’s north-central coast (NCC). To test the relevance of
176 these indicators to populations, we relate them to a few key biological data sets
177 that are representative of marine life within and outside NCC MPA.
178
- 179 3. To develop ocean-climate indicators, we selected, compiled and analyzed 16
180 well-known atmospheric and oceanographic measurements that represent key
181 large-scale drivers and regional attributes of the coastal physical environment.
182 These include drivers of ocean-climate variability from the tropical Pacific (e.g., El
183 Niño - Southern Oscillation) and north Pacific (e.g., Pacific Decadal Oscillation),
184 as well as regional atmospheric and ocean conditions such as wind stress, sea
185 surface temperature, salinity, and a novel time series of surface currents from the
186 State of California’s new HF radar array. While the indicators are based on
187 large- to regional-scale measurements, they have consequences for marine life
188 at the local (MPA) scale and thus are important to biological monitoring,
189 management evaluations, and adaptive management.
190
- 191 4. In this project, we designed and implemented seasonal indicators using a
192 multivariate statistical technique used to synthesize groups of related variables
193 known as Principal Component Analysis (PCA). PCA allows one to understand
194 relationships between similar variables taken from different locations, as well as
195 combine variables in a comprehensive and synthetic manner. We refer to this
196 compilation of variables as seasonal “Multivariate Ocean Climate Indicators”
197 (MOCI).
198
- 199 5. Our analysis of ocean conditions over the 21-year period leading up to MPA
200 establishment in the NCC study region indicates weakening of the ENSO cycle
201 resulting in fewer and less intense El Niño events, and a strengthening of sub-
202 arctic influences on the region including a major cooling represented by the
203 Pacific Decadal Oscillation (PDO). Corresponding to these changes, the
204 Northern Oscillation Index (NOI) strengthened, leading to enhanced upwelling-

205 favorable wind stress as well as air and ocean surface temperature cooling.
206 These conditions are conducive to population growth for species with temperate
207 or sub-arctic zoogeographic affinities, such as many fish species now protected
208 by MPAs. This indicates that population recovery may be enhanced by the
209 prevailing ocean conditions leading up to MPA implementation.

210

211 6. Corresponding to the recent increases in upwelling-favorable winds and
212 decreases in ocean temperature, phytoplankton biomass also increased in the
213 NCC study region. The positive trend observed in phytoplankton biomass could
214 be important for other marine life under study in NCC MPA as it indicates greater
215 biomass at the base of the food chain. MOCI also related well to seabird
216 productivity. We recommend additional tests of the applicability of MOCI to
217 populations, including populations studied during monitoring activities of central
218 coast MPA.

219

220 7. Our study supports a conclusion of enhanced sub-arctic influences and upwelling
221 intensification in north-central California over the past two decades, and that
222 these changes are contributing to greater lower trophic level biomass. Our
223 analyses provide context necessary to evaluate responses in local coastal
224 ecosystems to recent changes in fishing and other practices within MPA. Linking
225 changes in the MOCI to newly obtained biological observations from MPA
226 monitoring is warranted to separate the effects of ocean-climate variability from
227 changes in fishing and other anthropogenic pressures on these coastal
228 ecosystems and populations.

229

230 8. Regular updating of MOCI will be necessary to advance analyses of coupled
231 climate-ecosystem change and management evaluations in the NCC and other
232 study regions of California. It would also be of great value to consider the skill of
233 MOCI in predicting biological variables from NCC MPA monitoring once these
234 data are made accessible to the research and management communities.

235

236 9. Adaptive management of NCC MPA may be enhanced by the greater
237 understanding of ocean conditions revealed by MOCI and other indicators of
238 environmental variability. MOCI provide the environmental “backdrop” for the
239 evaluation of population change, thereby providing context with which to interpret
240 monitoring results within and outside MPA. If population changes within MPA
241 match those of control or reference sites, this could indicate that environmental
242 factors (as described by MOCI) are driving population changes. If population
243 changes do not match, this could indicate that management (protection) is having
244 a stronger impact. In this manner, managers may be able to ascribe the
245 statistical variation in populations to either environmental (ocean) conditions or
246 management actions.

247

248

249 **C. Final Revised Report**

250

251 **BASELINE CHARACTERIZATION OF ENVIRONMENTAL CONDITIONS**
252 **LEADING UP TO MARINE PROTECTED AREA ESTABLISHMENT IN**
253 **THE NORTH-CENTRAL COAST STUDY REGION**

254

255

256

257

258 William J. Sydeman^{1,2}, Sarah Ann Thompson^{1,3}, Marisol Garcia-Reyes¹,
259 and Mati Kahru²

260

261

¹Farallon Institute for Advanced Ecosystem Research
Petaluma, CA 94952

262

www.faralloninstitute.org

263

264

www.faralloninstitute2.wordpress.com

265

266

²Integrative Oceanography, Scripps Institution of Oceanography
La Jolla, CA 95060

267

268

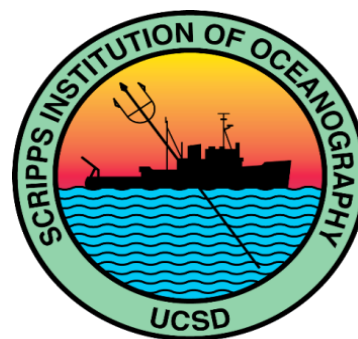
269

³Climate Impacts Group, University of Washington, Seattle, WA 98115

270

271

272



273

274

275

276

277

278

279

280

1 October 2013

281

282

283

284 1. Introduction

285 Ocean-climate variability has been shown to strongly affect marine life, including
286 plankton, fish, and top predators, with clear applications in fisheries, wildlife and
287 ecosystem management (Hjort, 1914; Cury et al., 2008; Carr et al., 2011). Compared to
288 many of the world's seas, the effects of ocean-climate variability on the California
289 Current ecosystem (CCE) have been particularly well-studied (Peña and Bograd, 2007).
290 This marine realm, situated off the west coast of Canada, the U.S., and Baja California,
291 Mexico, is affected by basin-scale atmospheric-oceanic coupling due to the combined
292 effects of El Niño Southern Oscillation events (ENSO; Lenarz et al., 1995; McPhaden et
293 al., 2006) and the decadal-scale North Pacific Gyre Oscillation (Di Lorenzo et al., 2008)
294 and Pacific Decadal Oscillation (PDO; Mantua et al., 1997). Regional coastal and
295 offshore upwelling, operating from daily to decadal time scales, also affect biotic
296 variability of the CCE (Huyer, 1983; García-Reyes and Largier, 2010, 2012).
297 Mechanistically, currents associated with tropical and extra-tropical transport bring
298 waters of varying characteristics into the system (Chelton et al., 1982). Subsequently,
299 regional upwelling and its vertical and offshore displacement operate on these water
300 masses, dispersing nutrients and plankton, which in turn determines primary and
301 secondary productivity (Checkley and Barth, 2009). Thus, to understand how climate
302 variability relates to marine life in the CCE, consideration of the interactive effects of
303 horizontal (currents) and vertical (upwelling) transport is required. Although a variety of
304 indicators are available to proxy these processes, rarely have they been combined in a
305 holistic manner to examine bio-physical interactions (but see Hemery et al., 2008).

306 The need for a comprehensive approach to ocean-climate indicators increased
307 recently when the State of California established a network of 124 Marine Protected
308 Areas (MPAs) and 15 special closures in which fisheries and other human activities
309 were either curtailed or eliminated entirely. This management began with the
310 implementation of 29 MPAs along the central California coast in 2007 followed by 25
311 MPAs along the central-northern coast in 2010. In 2012, 50 south coast and 20 north
312 coast MPAs were implemented. In total, ~852 mi² and ~16% of California's coastal
313 waters are now protected in no-take marine reserves and limited-take marine
314 conservation areas (www.dfg.ca.gov/mlpa). California's MPAs are located in coastal to
315 neritic habitats typically within three miles from shore, near offshore islands (such as the
316 Farallon Islands), and above major subsurface topographies (e.g., Monterey Canyon).
317 Since MPAs restrict fisheries and other human uses of marine species and habitats,
318 MPA implementation was controversial. Therefore, in conjunction with implementation,
319 an evaluation program designed to provide information on biotic responses to
320 reductions in fisheries mortality and other factors was initiated. Fieldwork for these
321 management-oriented evaluations began in 2008 along the central coast and in 2011
322 along the north-central coast.

323 Monitoring the outcome of reduced fishing when MPAs are established may be
324 complicated by environmental variability which can confound interpretations of biotic
325 change. For example, many of the focal *Sebastes* spp. respond to variation in large-
326 scale and local ocean climate with effects on growth (Black et al., 2010) and proxies of
327 reproductive success (Ralston et al., 2013). To place these recently obtained biological
328 observations in an environmental context, we designed and implemented a framework
329 for ocean-climate indicators for the central and north-central California Current by

330 combining a suite of well-known indicators using multivariate statistical procedures (see
331 also Mackas et al., 2007; Hemery et al., 2008). Our principal goal was to provide an
332 assessment of environmental conditions leading up to MPA establishment in the mid-
333 late 2000s. Because CCE biota respond to seasonal variation in environmental
334 conditions (e.g., Hooff and Peterson, 2006; Black et al., 2010, 2011; Thompson et al.,
335 2012), we produced indicators for intra-annual variability. The utility of complex
336 multivariate indicators can be challenged if they are difficult to interpret or do not
337 accurately represent known environmental variability (Rice and Rochet, 2005).
338 Therefore, based on the literature, we developed a series of *a priori* expectations to
339 evaluate multivariate indicators. These include El Niño conditions that affected the
340 region in 1992-1993, 1997-1998, 2003, and 2009-2010 (Bjorkstedt et al., 2010), the
341 warm-water non-El Niño event of 2005 (GRL Special Section, 2006), and strong La
342 Niña conditions in 1999 and 2008. These conditions have been well described in
343 previous publications, but to date there have been no attempts to create multivariate
344 ocean-climate indicators or evaluate how well these indicators represent such
345 variability. If indicators match known variability, arguably they would be interpretable
346 and representative, key attributes for useful and valid ecological indicators (Levin et al.,
347 2009). To test the utility of our multivariate ocean-climate indicators (hereafter MOCI,
348 see Hemery et al. 2008), we related them to two initial lower and upper trophic-level
349 biological indicators. We will provide a more comprehensive analysis of biological
350 responses to MOCI in a future report. Here, we focus on indicator development and a
351 description of environmental conditions over the 21-year period 1990-2010.

352

353 **2. Methods**

354 We focused data synthesis on 1990 through 2010 as this period followed the putative
355 regime shifts of 1989-1990 (Hare and Mantua, 2000) and 1976-1997 (McGowan et al.,
356 2003). Others have suggested another regime shift in 1998-1999 (Bond et al., 2003;
357 Peterson and Schwing, 2003), but the persistence of this shift remains equivocal. We
358 selected a total of 16 basin- (SOI, MEI, ONI, NPI, PDO, NPGO, NOI, and California
359 Current flow (two individual measurements)) and regional-scale (Upwelling Index, wind
360 stress, sea level, SST, salinity, surface air temperature, and precipitation) atmospheric
361 and oceanographic indicators for synthesis (Table 1, see below for descriptions). We
362 evaluated environmental conditions by exploring variability on different time scales.
363 When MPAs are established, fisheries mortality is reduced immediately. Therefore,
364 relatively short-term biotic responses are possible assuming rapidly responding
365 response parameters are monitored. In considering the potential for rapid biological
366 responses, we focused on understanding the status of the environment on seasonal,
367 interannual, and bi/triennial scales. However, while some rapid biological responses
368 are possible, long-lived species may not show short-term changes. This is certainly true
369 for the *Sebastes* spp. of interest in this ecosystem – changes in the populations of these
370 species are likely only on decadal scales. Therefore, in this context, we focused on
371 understanding trends in the environment and decadal-scale variability. Last, we
372 examine the potential for our multivariate ocean climate indicators to predict biological
373 responses by investigating relationships with two well-known biological indicators:

374 seabird reproductive success (Ainley et al., 1995; Sydeman et al., 2001, 2006, 2009)
 375 and chlorophyll-a concentrations (Kahru et al., 2012).

376

377 **2.1 Data**

378 **2.1.1 Indicators of Transport from the Tropics**

379 Indicators of the warm El Niño phase of the ENSO cycle are associated with strong
 380 advection from the tropics, whereas indicators of the cold La Niña phase reflect weak
 381 northward transport. We used three indicators for El Niño: one atmospheric, one
 382 oceanographic, and one multivariate indicator that includes both oceanographic and
 383 atmospheric variables. The Southern Oscillation Index (SOI), calculated as monthly
 384 fluctuations in sea level pressure between the Tahiti Low and Darwin, Australia High,
 385 was used as an indicator of the atmospheric drivers of ENSO. Prolonged negative
 386 values signify El Niño episodes while sustained positive values are associated with La
 387 Niña episodes. To present the SOI in phase with other variables, we reversed the sign
 388 of this indicator, such that positive values reflect El Niño and negative values reflect La
 389 Niña. Data were calculated by the Climate Analysis Section, National Center for
 390 Atmospheric Research, and were obtained from

391 <http://www.cgd.ucar.edu/cas/catalog/climind/SOI.signal.ascii>. The Oceanic Niño Index
 392 (ONI), a 3-month running mean of SST anomalies in the region 5°N-5°S, 120-170°W
 393 (Niño3.4), was used as an oceanographic manifestation of the ENSO cycle. The ONI is
 394 computed by the NOAA National Weather Service, Center for Climate Prediction. Data
 395 were obtained from

396 http://www.cpc.ncep.noaa.gov/products/analysis_monitoring/ensostuff/ensoyears.shtml.

397 The Multivariate ENSO Index (MEI), based on six observed variables over the tropical
 398 Pacific, was used as an indicator of the tropical oceanographic manifestation of the
 399 ENSO cycle (Wolter and Timlin, 1993). Negative values of the MEI represent the cold
 400 ENSO phase (La Niña), while positive MEI values represent the warm ENSO phase (El
 401 Niño). Data were obtained from NOAA's Earth System Research Laboratory at
 402 <http://www.esrl.noaa.gov/psd/enso/mei/table.html>.

403

404 **2.1.2 Indicators of Transport from the Extra-Tropics**

405 We selected the North Pacific Index (NPI), the area-weighted sea level pressure over
 406 the region 30°N-65°N, 160°E-140°W, as our atmospheric driver of transport from the
 407 North Pacific to the California Current. Data were calculated by the Climate Analysis
 408 Section, National Center for Atmospheric Research and were downloaded from
 409 <http://www.cgd.ucar.edu/cas/jhurrell/indices.data.html#npmon>. This variable provides
 410 an index of the strength and positioning of the Aleutian Low Pressure system, which in
 411 turn is expressed in large-scale ocean conditions in the North Pacific reflected in the
 412 Pacific Decadal Oscillation (PDO) and North Pacific Gyre Oscillation Index (NPGO).
 413 The NPGO index was downloaded from <http://eros.eas.gatech.edu/npgo/data/NPGO.txt>
 414 and emerges as the second EOF of Northeast Pacific sea-surface height anomalies (Di
 415 Lorenzo et al., 2008). Positive values also indicate a strong North Pacific gyre and
 416 advective transport from the north, whereas negative values indicate a weak gyre and
 417 decreased southward transport (Hooff and Peterson, 2006; Keister et al., 2011). We
 418 also used the PDO index, developed by Zhang et al. (1997), as an oceanographic index
 419 of sub-arctic influences on the CCE. Data were downloaded from the Joint Institute for

420 the Study of the Atmosphere and Ocean at the University of Washington. Methods and
421 details of computation are available at <http://jisao.washington.edu/pdo/PDO.latest>. The
422 PDO reflects SST for the entire North Pacific, including the CCE, at locations > 20°N.
423 Positive values of the PDO indicate warm SST along the eastern north Pacific and cool
424 SST over the central and western north Pacific.

425

426 **2.1.3 Indicators of Regional Upwelling**

427 The Northern Oscillation Index (NOI) provides an index of the strength and positioning
428 of the North Pacific High pressure system which, with the Continental Thermal Low,
429 drives the winds that cause upwelling in north-central California (Schwing et al., 2002).
430 The NOI is calculated by the Pacific Fisheries Environmental Laboratory, NOAA, based
431 on monthly fluctuations in the sea level pressure difference between the North Pacific
432 High and Darwin, Australia, Low thus also including variability from the tropics. NOI
433 data were downloaded from

434 http://www.pfeg.noaa.gov/products/PFEL/modeled/indices/NOI/noix_download.html.

435 The timing and amplitude of upwelling is proxied by the Bakun Upwelling Index (UI),
436 calculated by NOAA's Environmental Research Division, from estimates of the
437 magnitude of the offshore component of the Ekman transport driven by wind stress
438 (Schwing et al., 1996, 2006; Bograd et al., 2009). Positive values indicate upwelling
439 while negative values indicate downwelling. Methods and details of computation are
440 available from

441 [http://www.pfeg.noaa.gov/products/PFEL/modeled/indices/upwelling/NA/how_computed](http://www.pfeg.noaa.gov/products/PFEL/modeled/indices/upwelling/NA/how_computed.html)
442 [.html](http://www.pfeg.noaa.gov/products/PFEL/modeled/indices/upwelling/NA/how_computed.html). For this report we used UI indicators from 36°N 122°W and 39°N 125°W.

443

444

445 **2.1.4 Indicators of Local Current Flows**

446 Flow in the California Current in the sub-arctic region of the Northeast Pacific was
447 calculated by Howard Freeland of Fisheries and Oceans Canada using data collected
448 by Argo profiling floats (<http://www.argo.net/>; Freeland and Cummins, 2005). Positive
449 values indicate stronger flows whereas negative values indicate weaker flows. Surface
450 flow data were also collected by High-Frequency (HF) Radar (Barrick and Lipa, 1979)
451 off of Point Reyes, California, in conjunction with the Coastal Ocean Currents
452 Monitoring Program (COCMP; Halle and Largier, 2011), and a surface current flow
453 index was produced. Radial data from two standard range stations, BML1 (located at
454 Bodega Bay) and PREY (located at South Beach, Point Reyes) were combined using
455 standard CODAR data processing methods (Kaplan et al., 2005). The Point Reyes flow
456 index is defined in terms of four cells, each measuring approximately 14.6 km x 18.5 km
457 (270 km²) starting at the coast and extending approximately 51.2 km out to sea from
458 Point Reyes, including the area around Cordell Bank. The cell boundaries are defined
459 by lines of longitude and latitude spaced at 10-minute intervals between 123°0'W 38°0'N
460 and 123°40'W 38°10'N. Within each cell, an hourly-based total vector file was
461 processed to calculate daily and monthly average U (westward) and V (southward)
462 current values from all the vectors located within each cell. Here, we focus on the V
463 component. Negative values indicate current flow in a southward direction, but to put
464 this variable in phase with the others we reversed the sign, therefore positive values
465 indicate stronger surface flows to the south.

466

467 **2.1.5 Indicators of Local Atmospheric and Hydrographic Conditions**

468 We used alongshore wind stress as an index of upwelling-favorable winds in the region.
 469 García-Reyes and Largier (2010, 2012) calculated this variable based on wind speed
 470 and direction measured at NOAA buoys at Point Arena (39.2°N 124.0°W), Bodega Bay
 471 (38.2°N 123.3°W), San Francisco (37.8°N 122.8°W) and Half Moon Bay (37.4°N
 472 122.9°W). Negative values indicate wind stress in an upwelling-favorable equatorial
 473 direction, but for better interpretation of this variable we reversed the sign to make it in
 474 phase with other indicators. Details of the methodology can be found in García-Reyes
 475 and Largier (2010, 2012). Sea level measurements (mm), compiled by the National
 476 Water Level Observation Network (NWLON), were obtained from the Center for
 477 Operational Oceanographic Products and Services (CO-OPS; NOS, 2008). We used
 478 monthly data, which represent an average of daily values, from the San Francisco
 479 (37.8°N 122.5°W), Crescent City (41.4°N 124.1°W), and South Beach (41.5°N 124.1°W)
 480 sea level gauges. Methods and data were downloaded from the University of Hawaii
 481 Sea Level Center (<http://uhslc.soest.hawaii.edu/>). Local sea level also indexes
 482 upwelling and transport. Sea surface temperature data (SST; °C) were collected from
 483 the Farallon Islands shore station (37.7°N 123°W), NOAA buoys (Point Arena (39.2°N
 484 124.0°W), Bodega Bay (38.2°N 123.3°W), San Francisco (37.8°N 122.8°W), Half Moon
 485 Bay (37.4°N 122.9°W) and Monterey Bay (36.8°N 122.4°W)), and the Bodega Ocean
 486 Observing Node (BOON) program at the UC Davis Bodega Marine Lab (38.3°N
 487 123.1°W). Methods and data for the Farallon Islands shore station are available from
 488 http://shorestation.ucsd.edu/methods/index_methods.html. Buoy data were
 489 downloaded from the National Data Buoy Center (<http://www.ndbc.noaa.gov/>) and
 490 Bodega Marine Lab SST data were downloaded from
 491 http://bml.ucdavis.edu/boon/data_seatemp.html. Salinity data (psu) from the Farallon
 492 Islands (37.7°N 123°W) and the Bodega Marine Lab (38.3°N 123.1°W) were also
 493 compiled. Data were downloaded from
 494 ftp://ftp.iod.ucsd.edu/shore/active_data/farallon/salinity/ and
 495 http://bml.ucdavis.edu/boon/data_salinity.html, respectively. Air temperature (°C) was
 496 measured at the Bodega Marine Lab (BML; 38.3°N 123.1°W) in a weather box 40 m
 497 from the coastal bluff. Data were obtained from
 498 http://bml.ucdavis.edu/boon/data_airtemp.html. Daily temperatures were averaged to
 499 monthly values for analysis. Lastly, precipitation (cm) and air temperature (°C) data
 500 were downloaded from the National Climate Data Center, NOAA
 501 (<http://cdo.ncdc.noaa.gov/pls/plclimprod/somdmain.somdwrapper?datasetabbv=DS3220&countryabbv=&georegionabbv=&forceoutside>)
 502 for the sites Fort Ross (38.5°N 123.3°W), San Francisco (37.7°N 122.5°W), Pacifica
 503 (37.6°N 122.5°W), and Half Moon Bay (37.5°N 122.5°W).

505

506 **2.1.6 Lower Trophic Level Indicator**

507 We used a data set of regional satellite-derived chlorophyll-a (chl-a) combined from
 508 multiple sources into a consistent time series of spatial data sets (images) to achieve
 509 the longest temporal coverage possible. Methods for the compilation of this data set
 510 are described by Kahru et al. (2012). Briefly, long term measurements of phytoplankton
 511 biomass, proxied by estimates of chlorophyll-a, can be obtained *in situ* and by ocean

512 color satellites. However, as the life-span of a single satellite sensor is limited,
513 seamlessly merging ocean color observation data from multiple satellite sensors that
514 have different optical bands, sensitivities, noise patterns and overpass times
515 (Maritorena and Siegel, 2005) into a single unified time series remains a major
516 challenge (Gregg et al., 2009). For this study, Kahru et al. consolidated outputs from
517 four major ocean color sensors and created new algorithms to make output from these
518 sensors compatible with each other and with *in situ* chlorophyll-a data collected in the
519 region. To accomplish this task, Kahru et al. matched values from full-resolution Level-
520 2 satellite data (OCTS, SeaWiFS, MODIS-Aqua, and MERIS) with a data set of 10,050
521 near-surface *in situ* chlorophyll-a measurements taken from ships over the period 1996
522 through 2010. All satellite sensors showed strong positive correlations with *in situ* data
523 with the coefficient of determination (r^2) for the spatial matches ranging from 0.791
524 (SeaWiFS) to 0.864 (OCTS). At the same time, significant biases were observed
525 between *in situ* and satellite data. Kahru et al. minimized the differences and created
526 algorithms that were consistent with both *in situ* and satellite-based sensors. The
527 optimized algorithms were then applied to the daily Level-3 remote sensing data sets of
528 the four sensors and merged into unified daily chlorophyll-a data sets. The merged
529 daily data were then composited into monthly data sets. Chlorophyll-a concentration is
530 log-normally distributed. To account for this, we log transformed monthly chlorophyll-a
531 data before calculating a monthly average and subtracting the monthly average from
532 each log transformed monthly value to create anomalies.

533

534 **2.1.7 Upper Trophic Level Indicator**

535 Reproductive success for the seabirds common murre (*Uria aalge*), pigeon guillemot
536 (*Cephus columba*), Cassin's auklet (*Ptychoramphus aleuticus*), and Brandt's
537 cormorant (*Phalacrocorax penicillatus*) was studied at Southeast Farallon Island,
538 California, 37.7°N 123°W, by PRBO Conservation Science. Reproductive success was
539 the number of offspring departing the colony per breeding pair per year (Sydeman et al.,
540 2001). Data were available for 1971-2007 for all species except common murre, which
541 were available for 1972-2007. Seabird data were de-trended using quadratic regression
542 and the residuals were saved for further analysis.

543

544 **2.2 Data Processing and Statistical Analyses**

545 Monthly measurements of environmental conditions were expressed as anomalies
546 (monthly value – long-term monthly average; based on full length of time series, see
547 Table 1). To integrate measurements of each variable from different sites (i.e., seven
548 sites of measures of SST, four locations of wind stress measurements) we used
549 empirical orthogonal function/principal component analysis (PCA; Legendre and
550 Legendre, 1998). The unrotated first principal component (PC1) for each variable type
551 was extracted and retained for further analysis and evaluation. To test for trends in
552 univariate indicators, we conducted Spearman rank correlations on each variable over
553 time for each measurement site as well as for variable type PC1s. To test for
554 relationships between variables, we used Spearman rank cross-correlations. To create
555 seasonal MOCI, we used monthly values averaged across months for the following
556 seasons: winter (January-March), spring (April-June), summer (July-September) and
557 fall (October-December). Residuals of seasonal averages were calculated and used in

558 a PCA conducted on all oceanic and atmospheric variables except surface flow, by
559 season, for the years 1990-2010. The unrotated first principal component (MOCI1) for
560 each season was extracted and retained. The seasonal MOCI described above used
561 the full suite of climate variables, from large-scale indices to local-scale measurements.
562 We also generated two additional sub-groups of seasonal MOCI using PCA from (1)
563 only the large-scale climate indices and (2) only the regional-local measurements.
564 Subsequently, we cross-correlated these sub-groups with our original MOCI of the full
565 suite of large-scale as well as local climate variables to investigate similarities and
566 differences between these approaches. As we were primarily interested in
567 environmental conditions leading up to the growing season each year (~March-August),
568 we examined the cross-correlations of MOCI and the sub-groups for fall of year_{x-1} and
569 winter, spring, and summer of year_x. Last, we correlated the full-suite seasonal MOCI
570 with the de-trended biological indicators. For chlorophyll-a, we created an annual time
571 series by averaging monthly residuals from October to September. We used fall MOCI
572 of the previous year and winter, spring, and summer MOCI of the concurrent year to test
573 for temporal associations. The seabird residual data were synthesized using PCA and
574 the first principal component (PC1_{seabirds}) was saved for analyses. Seabird species
575 residual data and PC1_{seabirds} were tested against seasonal MOCI of the same year.

576

577 **3. Results**

578 **3.1 Status and Trends in Basin-Scale Indicators**

579 Results of spearman rank correlation tests for data trends are shown in Table 2. The
580 SOI, MEI, and ONI showed negative trends (Fig. 1), indicating a decrease in the
581 frequency and amplitude of El Niño events. 2010 values for the SOI and MEI were
582 particularly anomalous (almost 2x standard deviation), indicating a strong La Niña event
583 in that year. However, this followed a moderate El Niño from mid-2009 through early
584 2010. For extra-tropical indices, the NPI showed no trend (Fig. 2a) while the PDO
585 decreased (indicating cooling of the eastern Pacific, Fig. 2b). The NPGO increased
586 (indicating greater gyre transport) with a distinct step from negative to mostly positive
587 values in early 1998 (Fig. 2c) and showed a strong period of transport from early 1999
588 to early 2003, which corresponds to negative values of the PDO during the same time
589 period. The NPGO has been largely positive since early 2010, corresponding to a
590 negative PDO. Changes in the NPGO and PDO during the El Niño of 2009 were not
591 particularly noteworthy (i.e., well within 1 s.d. of the mean).

592

593 **3.2 Status and Trends in Regional Upwelling Indicators**

594 The NOI increased in the study period though the overall rate of change was small
595 (Table 2, Fig. 3a). The NOI was strongly negative (indicating a weak North Pacific
596 High) in early 2010, corresponding to the 2009-2010 El Niño, but rebounded to normal
597 levels later in the year. The NOI was particularly high from mid-2007 to early 2009, and
598 was low but not outside 1 s.d. of the mean from late 2002 through 2006. Similar to the
599 NOI, the UI at 36°N and 39°N had a slight, but significantly positive trend (Table 2, Fig.
600 3b). Strong negative values in late 2009 indicate downwelling during the 2009-2010 El
601 Niño, and the highest values were observed from 1999 through 2002.

602

603 **3.3 Status and Trends in Regional and Local-Scale Current Indicators**

604 There was no trend in the flow of the California Current based on Argo measurements,
605 2002-2010 (Table 2, Fig. 4a). An anomalously low flow rate was detected, however, for
606 mid-late 2004 and early-mid 2010. The largest flow was observed from mid 2007 to late
607 2008. Local flow of surface currents off Point Reyes were generally in the positive
608 (increasing) direction (Fig. 4b) though only for cell 2 was the trend significant (Table 2).
609 Local surface currents were highly variable within and between months and years. A
610 peak in the surface flow off Point Reyes was observed in 2004 (opposite to flow in the
611 California Current), with another increase in 2007-2008 (corresponding to high
612 California Current flows).

613

614 **3.4 Status and Trends in Regional Wind and Hydrographic Indicators**

615 Clear trends were observed for wind stress and SST (Table 2, Fig. 5a,b). Wind stress
616 increased significantly at all sites and was particularly strong in 2008 but decreased in
617 2009. SST decreased significantly at 4 of 7 locations over the 21-year period and was
618 particularly low for the period 2007-2010. The only significant change in sea level,
619 however, was decreasing sea level at Crescent City (Table 2, Fig. 5c). Sea level was
620 elevated in late 2009, corresponding to the El Niño event at that time, but has since
621 decreased. There were no significant trends for salinity (Fig. 5d). Corresponding to the
622 cold SST, salinity in recent years has also been elevated but decreased from 2007-
623 2010 and was not outside average values in most of 2009 and 2010.

624

625 **3.5 Status and Trends in Regional Air Temperature and Precipitation Indicators**

626 Air temperature represented by five sites showed a decreasing trend (Table 2, Fig. 6a)
627 with the exception of Pacifica where the trend was positive and non-significant. Air
628 temperature was generally low from 2008-2010. There was no overall trend for
629 precipitation (Fig. 6b).

630

631 **3.6 Variable-Specific Multivariate Indicators**

632 Within key climate variable types, creating linear combinations of sites using PCA was
633 supported and interpretable. Eigenvalues for the first principal component (PC1) were
634 >3 for surface flow at Point Reyes, wind stress, SST, air temperature and precipitation
635 (Table 3a). Within each of these variables, loadings for different sites were similar
636 (Table 3b). For example, loadings for SST, which include data from seven sites, ranged
637 from 0.338 (Monterey Bay) to 0.407 (Farallon Islands). Similarly, loadings for wind
638 stress for four sites ranged from 0.465 (San Francisco) to 0.514 (Half Moon Bay). This
639 reveals strong covariance between sites as well as similar contributions from each site
640 to each multivariate index, thus justifying our approach. Trends in multivariate indices
641 for upwelling, wind stress, and SST confirmed the pattern seen in univariate analyses of
642 increasing NOI, increasing upwelling-favorable wind stress, and decreasing SST in the
643 region (Table 2).

644

645 **3.7 Correlations Among Physical Environmental Indicators**

646 Correlations between environmental indicators are shown in Table 4. These
647 correlations are based on monthly data and are therefore highly autocorrelated. Due to
648 this concern, we did not attempt to assign statistical significance to these correlations,
649 but instead highlight associations with $\rho > 0.5$. Not surprisingly, the three sub-tropical

650 indices (SOI, MEI, ONI) were well related to one another. The NOI was related to the
 651 upwelling index, surface flow at Point Reyes, wind stress, SST, and sea level. SST and
 652 salinity were negatively correlated, while SST and air temperature were positively
 653 associated. Notably, at the $\rho > 0.5$ level, the NPI, NPGO, and California Current flow
 654 were unrelated to any other indicators.

655

656 **3.8 Development of Seasonal Multivariate Ocean-Climate Indicators (MOCI)**

657 Due to seasonal variation, we used PCA to create linear combinations of all physical
 658 variables within seasons (Table 5). There were distinct differences in the MOCI created
 659 for winter (JFM) and spring (AMJ) versus summer (JAS) and fall (OND). The
 660 eigenvalues for winter and spring were >18 whereas summer and fall were <14 ; this
 661 related to greater variance explained in the first two seasons (56% and 53%,
 662 respectively) compared to the latter seasons (38% and 40%, respectively; Table 5a).
 663 The second principle components for each seasonal MOCI were balanced with
 664 eigenvalues >4 , and the variance explained by each was $\sim 13.5\%$. MOCI1-winter
 665 appeared to primarily be explained by a weak NOI (weak North Pacific High) and
 666 positive sea level and SST (Table 5b, Fig. 7a). We interpret MOCI1-winter as an index
 667 of wintertime atmospheric pressure and upwelling. MOCI2-winter was explained
 668 primarily by variation in precipitation (Table 5b); we therefore interpret MOCI2-winter as
 669 an indicator of local winter atmospheric conditions, including the PDO. MOCI1-spring
 670 appeared to be explained primarily by negative upwelling at 39°N and positive sea level
 671 and SST (Table 5b, Fig. 7b). Thus, we interpret MOCI1-spring as an index of PDO-
 672 driven variation in sea level and SST (high and warm). MOCI2-spring was explained
 673 primarily by variation in SOI (positive) and NPI (negative; Table 5b), as well as
 674 precipitation. MOCI1-summer appeared to be explained primarily by positive sea level,
 675 SST, and air temperature (Table 5b, Fig. 7c). We interpret MOCI1-summer as an index
 676 of temperature. MOCI2-summer was explained primarily by weak (positive) wind stress
 677 coupled with temperature and precipitation (Table 5b). Last, MOCI1-fall appeared to be
 678 related to the PDO (positive), NOI (negative), weak wind stress, and positive sea level
 679 and SST (Table 5b, Fig. 7d), reflecting weak upwelling conditions. MOCI2-fall was
 680 explained primarily by variation in SOI, MEI, and ONI (Table 5b); therefore, we interpret
 681 MOCI2-fall as an indicator of ENSO conditions.

682

683 **3.9 Trends in MOCI**

684 Trends in seasonal MOCI are depicted in Fig. 8. MOCI1-winter showed strong
 685 upwelling in 1990 and 2007-2008, and particularly weak upwelling in 1992, 1995, 1998,
 686 2005 and 2010. The overall trend for MOCI1-winter is for more upwelling interannually.
 687 MOCI1-spring showed elevated sea level and SST in 1992, 1998, and 2005-2006, and
 688 low sea level and cold SST in 1991, 1999, 2001-2002 and 2008. The trend for MOCI1-
 689 spring is for lower sea level and SST through time. MOCI1-summer showed warming in
 690 1997 and 2004 and cooling in 1994, 1996, 2000-2001 and 2010. The overall trend for
 691 MOCI1-summer is for ocean cooling, but this is driven largely by 2010. MOCI1-fall
 692 showed weak upwelling in 1992, 1997, and 2002, and particularly strong upwelling in
 693 1990, 1998, 2000, and 2007. There is no overall trend in upwelling for MOCI1-fall. The
 694 full MOCI time series is shown in Fig. 9. Years generally categorized as subtropical,
 695 warm, and rainy with weak winds and upwelling are 1992-1998 and 2003-2007. The

696 pronounced 1997-1998 ENSO shift is clearly seen. Years generally categorized as sub-
 697 arctic and cold with strong winds and upwelling are 1990-1991, 1999-2002, and 2007-
 698 2011.

699

700 **3.10 Correlations between MOCI, Large-Scale Climate Indices, and Local** 701 **Measurements**

702 Seasonal sub-groups of MOCI produced from large-scale climate indices only and
 703 regional-local measurements only, and the original MOCI from all variables combined
 704 did not vary substantially from one another and were highly correlated (Table 6).

705

706 **3.11 Status and Trends of Biological Indicators**

707 Chlorophyll has increased since 1997 (Fig. 10a; $n = 168$, $\rho = 0.41$, $p\text{-value} < 0.001$).
 708 There was no trend in reproductive success for pigeon guillemot or Cassin's auklet (Fig.
 709 10b,c), but common murre had a negative trend (Fig. 10d; $n = 36$, $\rho = -0.29$, $p\text{-value} =$
 710 0.085) and Brandt's cormorant had a positive trend (Fig. 10e; $n = 37$, $\rho = 0.47$, $p\text{-}$
 711 $\text{value} = 0.003$); both of these trends were eliminated using quadratic regression.
 712 $PC1_{\text{seabirds}}$ explained 65% of the variability in the reproductive success of these four
 713 species (Fig. 10f, eigenvalue = 2.61), and the loadings were largely equal between
 714 species (range = 0.45-0.53).

715

716 **3.12 Correlations between Environmental and Biological Indicators**

717 There were no significant relationships between seasonal MOCI and chlorophyll-a
 718 concentrations, but there were several correlations between seasonal MOCI and
 719 seabird variables. MOCI1-spring was significantly correlated with reproductive success
 720 of all seabird species as well as $PC1_{\text{seabirds}}$ (Table 7, Fig. 11). All relationships between
 721 seasonal MOCI and seabird reproductive success (including $PC1_{\text{seabirds}}$) were negative
 722 indicating reduced breeding success with increasing MOCI values. MOCI-spring
 723 explained 28%, 76%, 43%, and 37% of the variation in the breeding success of Cassin's
 724 auklet, common murre, pigeon guillemot, and Brandt's cormorant, respectively, and
 725 59% of the variation in $PC1_{\text{seabirds}}$.

726

727 **4. Discussion**

728 Disentangling the effects of climate variability and fishing on coastal ecosystems is a
 729 challenge as both factors occur simultaneously and interact to affect food webs and
 730 biological populations (Link et al., 2002; Hsieh et al., 2008; Kenny et al., 2009; Kirby et
 731 al., 2009). As MPA designations are controversial, robust evaluations of the goals of
 732 MPAs in protecting and restoring ecosystems are needed. We implemented this study
 733 to aid in the interpretation and evaluation of ecological and biological changes within
 734 and outside newly established MPAs in the central California Current. Our primary
 735 goals were to design multivariate ecosystem indicators that capture the ocean-climate
 736 processes which affect a variety of marine life, and provide understanding of temporal
 737 environmental trends and variability in conditions during the two decades leading up to
 738 MPA designation.

739

740 **4.1 Indicator Design and Development**

741 To derive a description of environmental variability through time, we created seasonal,
742 multivariate indicators of environmental conditions based on linear combinations of 16
743 well-known atmospheric and oceanographic indicators. In part, we modeled this work
744 after Hemery et al. (2008) and Kenny et al. (2009), who took a similar approach to
745 investigating coupled climate and ecosystem change in the Bay of Biscay, France, and
746 the North Sea, respectively. Hemery et al. used 11 climate variables over four seasons
747 (i.e., 44 variables described each year) to create their “Multivariate Ocean-Climate
748 Index”, and compared it to the major climate index of their region, the winter North
749 Atlantic Oscillation (wNAO). Hemery et al. used SST, air temperature, precipitation, and
750 wind variables, as we did, but they did not integrate measurements of salinity, surface
751 currents, or sea level. We used all of these variables, as well as a variety of basin-scale
752 atmospheric and oceanographic indices (listed above), to create season-specific
753 Multivariate Ocean Climate Indices (“MOCI”; winter (January-March), spring (April-
754 June), summer (July-September), and fall (October-December)). As most biological
755 processes and populations in the California Current are dependent on seasonal
756 variation in environmental conditions (e.g., Abraham and Sydeman, 2004; Black et al.,
757 2010, 2011), we surmised that deriving seasonal MOCI would be the most appropriate
758 way to examine physical – biological interactions in this region.

759
760 The seasonal MOCI time series we derived is shown in Fig. 9. By placing the seasonal
761 values in sequence, we can verify whether these indicators reflect known transitions in
762 environmental conditions, for example, those occurring during well-documented ENSO
763 events in the eastern tropical Pacific. The strongest El Niño on record transitioned to
764 one of the strongest La Niña events on record from 1997 to 1999 (Chavez et al., 1999).
765 According to our MOCI, the 1997-98 El Niño reached its peak in summer 1997 and
766 transitioned to La Niña during the spring and summer of 1998. This seasonality is
767 temporally matched to physical, chemical, and biological changes in the tropical Pacific
768 and central California (Chavez et al., 2002). Similarly, a weaker, though still significant
769 transition to an El Niño event occurred from 1991 to 1992. Our seasonal MOCI indicate
770 that this transition occurred during from winter 1991 through spring/summer 1991 and
771 peaked in winter/spring 1992. This transitional period also matched reported changes
772 in biogeochemical attributes of the tropical Pacific (Barber et al., 1996) and central
773 California (Chavez, 1996) at that time. More recently, a modest El Niño occurred with
774 the peak observed in our seasonal MOCI in winter 2010 (MEI;
775 <http://www.esrl.noaa.gov/psd/enso/mei/table.html>). That MOCI match the timing of
776 major and well-known basin-scale oceanographic transitions provides confidence that
777 the environmental measurements selected, as well as statistical procedures used, result
778 in MOCI that accurately represent the environmental conditions in the region.

779

780 **4.2 Trends in Environmental Conditions**

781 The state of a marine ecosystem is a function of the forces acting upon it at various
782 temporal and spatial scales. To assess trends in environmental conditions for the north-
783 central California coastal region, we summarized indicators for the period 1990-2010
784 and selected basin-, regional-, and local-scale indicators. We selected 1990 as our
785 cutoff due to a putative “regime shift” in environmental conditions and ecosystem status
786 that occurred at that time (Hare and Mantua, 2000; Sydeman et al., 2001). Since 1990,

787 the primary trend in the environment of north-central coastal California can be
788 summarized as follows: (1) a general weakening of sub-tropical influences on the
789 system, illustrated by declining trends in the SOI, MEI, and ONI, (2) a general
790 strengthening of sub-arctic influences, shown by cooling of the PDO and increases in
791 the NPGO, and (3) increasing regional-scale upwelling, documented by a stronger NOI
792 and UI at both 36°N and 39°N. We found no change in currents on either the large-
793 (California Current flow) or local- (surface flow at Point Reyes) scale, probably because
794 the time series for these variables were too short (2002-2010), although flow rates were
795 generally positive as would have been expected under generally increasing sub-arctic
796 influences. Upwelling intensification over the period was supported by observations of
797 significantly increasing wind stress (4 of 4 buoys) and decreasing SST (4 of 7 buoys).
798 PC1 values of wind stress and SST reflective of the entire region confirmed these
799 patterns of change. Interestingly, despite decreasing SST, we did not observe trends in
800 salinity or sea level. Three of five sites showed decreasing air temperature which may
801 be related to changes in ocean temperature. In short, changes in sub-arctic influences,
802 particularly the NPGO, and regional upwelling and ocean temperature have made the
803 environment more temperate in nature.

804

805 **4.3 Relationships between Indicators**

806 Correlations between indicators (Table 4) confirm that three main factors appear to
807 affect environmental conditions in the marine environment of north-central California.
808 Highlights of robust correlations ($\rho > 0.5$) show clusters of associations amongst
809 ENSO-related variables (MEI, SOI, ONI) as well as their relationships to the PDO and
810 NOI. The ENSO indicators were related to sea level and SST, but not at $\rho > 0.5$.
811 PDO-related associations were strong with sea level and SST as well as air
812 temperature. The correlations between PDO and SST and sea level were positive,
813 indicating a possible mechanistic connection between PDO and transport (indicated by
814 sea level); SST and sea level were also strongly connected. The last cluster of
815 correlations was associated with the NOI, including positive associations with surface
816 flow and wind stress (indicative of upwelling) and negative associations with SST and
817 sea level. The NOI-related cluster apparently reflects regional upwelling and local
818 conditions. Salinity was negatively correlated with sea level and SST, as expected if
819 sea level and SST are driven by upwelling. These clusters of associations suggest that
820 models of physical-biological interactions could be well represented by no less than
821 three basin-scale indicators, one for influence from the sub-tropics (MEI), one for
822 influence from the sub-arctic (PDO), and one for upwelling (NOI). Models of physical-
823 biological interactions at the regional or local scale would be well represented by at
824 least one indicator, and we would suggest sea level for this purpose as it integrates all
825 large-scale factors. Moreover, the strongest correlations we found were between sea
826 level and the NOI ($\rho = -0.76$) and sea level and SST ($\rho = 0.70$). As previously
827 suggested (Sydeman and Thompson, 2010), sea level is perhaps the best univariate
828 indicator available for use in environmental and ecosystem assessments. Sea level
829 was well correlated with our seasonal MOCI (Table 5).

830

831 **4.4 Environmental Conditions Immediately Preceding MPA Establishment**

832 Seasonal MOCI indicate substantial transitions and variability in the years leading up to
833 MPA establishment along the central California coast in 2007 and north-central region in
834 2010 (Fig. 9). The years 2004-2006 (time preceding establishment of MPA in the NCC)
835 were characterized by poor upwelling and generally warm conditions. The year 2008
836 was characterized by strong upwelling and cold SST in the winter and especially spring,
837 which transitioned to “normal” conditions (within 1 s.d. of the average PC value) in
838 summer and fall and continued through 2009. Winter 2010 was characterized by strong
839 El Niño conditions, comparable to winter 1998, however, this event was relatively short-
840 lived and by summer 2010 La Niña conditions with strong upwelling and low SST
841 prevailed. Bjorkstedt et al. (2010) describe similar transitions in the entire CCE in 2009
842 and 2010. By fall 2010, conditions were within normal bounds.

843

844 **4.5 Linking Environmental and Biological Indicators**

845 As noted above, MOCI reflected well-documented environmental transitions and
846 variability, and we are therefore confident that we selected and processed appropriate
847 variables using multivariate procedures. However, it is clear that patterns of variability
848 of a lower (chl-a) trophic level indicator do not match the patterns of variability in MOCI,
849 neither seasonally nor from an interannual perspective (Fig. 10a). We found an
850 increasing chl-a trend which may be related to positive trends in increasing wind stress
851 (and decreasing SST; Table 2; Wilkerson et al., 2006), but found no correlations
852 between seasonal MOCI and de-trended chl-a abundance, indicating no associations
853 on the interannual time scale. Moreover, a peak in chl-a was observed in the 2004-
854 2006 period when MOCI generally indicated warm conditions with weak upwelling.
855 Measuring bulk chl-a does not provide information on phytoplankton community
856 composition, which may explain why correlations with MOCI were elusive since
857 phytoplankton species respond differently to transport, upwelling, and variation in local
858 hydrographic conditions (Chavez et al., 2011). In support of this idea, the seabird
859 indicators based on productivity of individual species were strongly associated with
860 seasonal MOCI, with spring in particular explaining a significant proportion of the
861 variability in species-specific and combined seabird breeding success. Seabird
862 breeding success in itself is an integration of a several parameters including the number
863 of eggs produced per nest (clutch size), the proportion of eggs hatched, and the
864 proportion of hatched chicks raised to independence (for interannual variation in these
865 parameters see Sydeman et al., 2001). Seabird breeding success has been presented
866 previously as an indicator of prey abundance (Cairns, 1987; Piatt et al., 2007),
867 specifically mesozooplankton (e.g., krill) and small forage fish used for offspring
868 production (Sydeman et al., 2013). Therefore, the strong connection between seabird
869 breeding success and spring MOCI suggests that the MOCI may also be an indicator of
870 the coastal food webs that seabirds are dependent upon. More importantly, this
871 provides support for our approach in both designing and implementing MOCI, and for
872 potential application in assessing biotic changes in MPAs. The seabird correlations also
873 support our contention that the lack of correlation with bulk chl-a may be due to poor
874 information content about which species of phytoplankton are represented in the chl-a
875 values obtained via satellite remote-sensing.

876

877 **5. Conclusion**

878 We designed and implemented multivariate indicators of ocean climate (MOCI) for the
879 north-central study region based on processes known to affect populations and
880 ecosystem dynamics there (transport from the south and north and regional upwelling).
881 The seasonal MOCI represented environmental variability well and show promise for
882 understanding physical-biological interactions in the system. MOCI can be used to put
883 biological findings in the context of broader environmental variability.
884

885 **6. Acknowledgements**

886 For data contributions to this project, we thank John Largier and Marcel Losekoot
887 (Bodega Marine Lab) for providing information of surface currents, Jim Johnstone
888 (JISAO, University of Washington) for providing data on air temperature and
889 precipitation, Howard Freeland (Fisheries and Oceans Canada) for providing data on
890 California Current flow rates from the Argo array, and PRBO for data on seabird
891 breeding success. We thank the State of California's MPA Monitoring Enterprise, the
892 Ocean Science Trust, California Sea Grant, and the National Science Foundation
893 (California Current Ecosystem Long-term Ecological Research program) for financial
894 support.
895

896
897
898
899
900
901
902
903
904
905
906
907
908
909
910
911
912
913
914
915
916
917
918
919
920
921
922
923
924
925
926
927
928
929
930
931
932
933
934
935
936
937
938
939
940

7. Literature Cited

- Abraham, C.L., Sydeman, W.J., 2004. Ocean climate, euphausiids and auklet nesting: inter-annual trends and variation in phenology, diet and growth of a planktivorous seabird, *Ptychoramphus aleuticus*. Marine Ecology Progress Series 274, 235-250.
- Ainley, D.G., Sydeman, W.J., Norton, J., 1995. Upper trophic level predators indicate interannual negative and positive anomalies in the California Current food web. Marine Ecology Progress Series 118, 69-79.
- Barber, R.T., Sanderson, M.P., Lindley, S.T., Chai, F., Newton, J., Trees, C.C., Foley, D.G., Chavez, F.P., 1996. Primary productivity and its regulation in the equatorial Pacific during and following the 1991-1992 El Niño. Deep-Sea Research Part II 43, 933-969.
- Barrick, D.E., Lipa, B.J., 1979. A compact transportable HF radar system for directional coastal wave field measurements. In Earle, M.D., Malahoff, A., (Eds.), Ocean Wave Climate. Plenum Press, Plenum, New York, pp. 153-201
- Bjorkstedt, E.P., Goericke, R., McClatchie, S., Weber, E., Watson, W., Lo, N., Peterson, B., Emmett, B., Peterson, J., Durazo, R., Gaxiola-Castro, G., Chavez, F., Pennington, J.T., Collins, C.A., Field, J., Ralston, S., Sakuma, K., Bograd, S.J., Schwing, F.B., Xue, Y., Sydeman, W.J., Thompson, S.A., Santora, J.A., Largier, J., Halle, C., Morgan, S., Kim, S.Y., Merkens, K.P.B., Hildebrand, J.A., Munger, L.M., 2010. State of the California Current 2009-2010: Regional variation persists through transition from La Niña to El Niño (and back?). California Cooperative Oceanic Fisheries Investigations Report 51, 39-69.
- Black, B.A., Schroeder, I.D., Sydeman, W.J., Bograd, S.J., Lawson, P.W., 2010. Wintertime ocean conditions synchronize rockfish growth and seabird reproduction in the central California Current ecosystem. Canadian Journal of Fisheries and Aquatic Sciences 67, 1149-1158.
- Black, B.A., Schroeder, I.D., Sydeman, W.J., Bograd, S.J., Wells, B.K., Schwing, F.B., 2011. Winter and summer upwelling modes and their relevance to climate impacts and ecological response in the California Current Ecosystem. Global Change Biology 17, 2536-2545.
- Bograd, S.J., Schroeder, I., Sarkar, N., Qiu, X.M., Sydeman, W.J., Schwing, F.B., 2009. Phenology of coastal upwelling in the California Current. Geophysical Research Letters 36, L01602.
- Bond, N.A., Overland, J.E., Spillane, M., Stabeno, P.J., 2003. Recent shifts in the state of the North Pacific. Geophysical Research Letters 30, 2183.
- Cairns, D.K., 1987. Seabirds as indicators of marine food supplies. Biological Oceanography 5, 261-271.
- Carr, M.H., Woodson, C.B., Cheriton, O.M., Malone, D., McManus, M.A., Raimondi, P.T., 2011. Knowledge through partnerships: integrating marine protected area monitoring and ocean observing systems. Frontiers in Ecology and the Environment 9, 342-350.
- Chavez, F.P., 1996. Forcing and biological impact of onset of the 1992 El Niño in central California. Geophysical Research Letters 23, 265-268.

- 941 Chavez, F.P., Strutton, P.G., Friederich, G.E., Feely, R.A., Feldman, G.C., Foley, D.G.,
942 McPhaden, M.J., 1999. Biological and chemical response of the Equatorial
943 Pacific Ocean to the 1997-98 El Niño. *Science* 286, 2126-2131.
- 944 Chavez, F.P., Pennington, J.T., Castro, C.G., Ryan, J.P., Michisaki, R.P., Schlining, B.,
945 Walz, P., Buck, K.R., McFadyen, A., Collins, C.A., 2002. Biological and chemical
946 consequences of the 1997-1998 El Niño in central California waters. *Progress in*
947 *Oceanography* 54, 205-232.
- 948 Chavez, F.P., Messie, M., Pennington, J.T., 2011. Marine primary production in relation
949 to climate variability and change. *Annual Review of Marine Science* 3, 227-260.
- 950 Checkley, D.M., Barth, J.A., 2009. Patterns and processes in the California Current
951 System. *Progress in Oceanography* 83, 49-64.
- 952 Chelton, D.B., Bernal, P.A., McGowan, J.A., 1982. Large-scale interannual physical and
953 biological interactions in the California Current. *Journal of Marine Research* 40,
954 1095-1125.
- 955 Cury, P.M., Shin, Y.J., Planque, B., Durant, J.M., Fromentin, J.M., Kramer-Schadt, S.,
956 Stenseth, N.C., Travers, M., Grimm, V., 2008. Ecosystem oceanography for
957 global change in fisheries. *Trends in Ecology & Evolution* 23, 338-346.
- 958 Di Lorenzo, E., Schneider, N., Cobb, K.M., Franks, P.J.S., Chhak, K., Miller, A.J.,
959 McWilliams, J.C., Bograd, S.J., Arango, H., Curchitser, E., Powell, T.M., Riviere,
960 P., 2008. North Pacific Gyre Oscillation links ocean climate and ecosystem
961 change. *Geophysical Research Letters* 35, L08607.
- 962 Freeland, H.J., Cummins, P.F., 2005. Argo: A new tool for environmental monitoring
963 and assessment of the world's oceans, an example from the NE Pacific.
964 *Progress in Oceanography* 64, 31-44.
- 965 García-Reyes, M., Largier, J., 2010. Observations of increased wind-driven coastal
966 upwelling off central California. *Journal of Geophysical Research* 115, C04011.
- 967 García-Reyes, M., Largier, J.L., 2012. Seasonality of coastal upwelling off central and
968 northern California: New insights, including temporal and spatial variability.
969 *Journal of Geophysical Research* 117, C03028.
- 970 Gregg, W.W., Casey, N.W., O'Reilly, J.E., Esaias, W.E., 2009. An empirical approach to
971 ocean color data: Reducing bias and the need for post-launch radiometric re-
972 calibration. *Remote Sensing of Environment* 113, 1598-1612.
- 973 GRL Special Section. 2006. Warm ocean conditions in the California Current in
974 spring/summer 2005: Causes and consequences. *Geophysical Research Letters*
975 33(22).
- 976 Halle, C.M., Largier, J.L., 2011. Surface circulation downstream of the Point Arena
977 upwelling center. *Continental Shelf Research* 31, 1260-1272.
- 978 Hare, S.R., Mantua, N.J., 2000. Empirical evidence for North Pacific regime shifts in
979 1977 and 1989. *Progress in Oceanography* 47, 103-145.
- 980 Hemery, G., D'Amico, F.D., Castege, I., Dupont, B., D'Elbee, J., Lalanne, Y., Mouches,
981 C., 2008. Detecting the impact of oceano-climatic changes on marine
982 ecosystems using a multivariate index: The case of the Bay of Biscay (North
983 Atlantic-European Ocean). *Global Change Biology* 14, 27-38.
- 984 Hjort, J., 1914. Fluctuations in the great fisheries of northern Europe viewed in the light
985 of biological research. *Rapport et Proces-verbaux des Reunions, Conseil*
986 *International pour l'Exploration de la Mer* 20, 1-228.

- 987 Hooff, R.C., Peterson, W.T., 2006. Copepod biodiversity as an indicator of changes in
988 ocean and climate conditions of the northern California current ecosystem.
989 *Limnology and Oceanography* 51, 2607-2620.
- 990 Hsieh, C.H., Reiss, C.S., Hewitt, R.P., Sugihara, G., 2008. Spatial analysis shows that
991 fishing enhances the climatic sensitivity of marine fishes. *Canadian Journal of*
992 *Fisheries and Aquatic Sciences* 65, 947-961.
- 993 Huyer, A., 1983. Coastal upwelling in the California Current System. *Progress in*
994 *Oceanography* 12, 259-284.
- 995 Kahru, M., Kudela, R.M., Manzano-Sarabia, M., Mitchell, B.G., 2012. Trends in the
996 surface chlorophyll of the California Current: Merging data from multiple ocean
997 color satellites. *Deep-Sea Research Part II*, 77–80, 89–98.
- 998 Kaplan, D.M., Largier, J., Botsford, L.W., 2005. HF radar observations of surface
999 circulation off Bodega Bay (Northern California, USA). *Journal of Geophysical*
1000 *Research - Oceans* 110, C10020.
- 1001 Keister, J.E., Di Lorenzo, E., Morgan, C.A., Combes, V., Peterson, W.T., 2011.
1002 Zooplankton species composition is linked to ocean transport in the Northern
1003 California Current. *Global Change Biology* 17, 2498-2511.
- 1004 Kenny, A.J., Skjoldal, H.R., Engelhard, G.H., Kershaw, P.J., Reid, J.B., 2009. An
1005 integrated approach for assessing the relative significance of human pressures
1006 and environmental forcing on the status of Large Marine Ecosystems. *Progress*
1007 *in Oceanography* 81, 132-148.
- 1008 Kirby, R.R., Beaugrand, G., Lindley, J.A., 2009. Synergistic effects of climate and
1009 fishing in a marine ecosystem. *Ecosystems* 12, 548-561.
- 1010 Legendre, P., Legendre, L., 1998. *Numerical Ecology*. Elsevier, Amsterdam.
- 1011 Lenarz, W.H., Ventresca, D.A., Graham, W.M., Schwing, F.B., Chavez, F., 1995.
1012 Explorations of El Niño events and associated biological population dynamics off
1013 central California. *California Cooperative Oceanic Fisheries Investigations*
1014 *Reports* 36, 106-119.
- 1015 Levin, P.S., Fogarty, M.J., Murawski, S.A., Fluharty, D., 2009. Integrated Ecosystem
1016 Assessments: Developing the scientific basis for ecosystem-based management
1017 of the ocean. *PLoS Biology* 7, 23-28.
- 1018 Link, J.S., Brodziak, J.K.T., Edwards, S.F., Overholtz, W.J., Mountain, D., Jossi, J.W.,
1019 Smith, T.D., Fogarty, M.J., 2002. Marine ecosystem assessment in a fisheries
1020 management context. *Canadian Journal of Fisheries and Aquatic Sciences* 59,
1021 1429-1440.
- 1022 Mackas, D.L., Batten, S., Trudel, M., 2007. Effects on zooplankton of a warmer ocean:
1023 Recent evidence from the Northeast Pacific. *Progress in Oceanography* 75, 223-
1024 252.
- 1025 Mantua, N.J., Hare, S.R., Zhang, Y., Wallace, J.M., Francis, R.C., 1997. A Pacific
1026 interdecadal climate oscillation with impacts on salmon production. *Bulletin of the*
1027 *American Meteorological Society* 78, 1069-1079.
- 1028 Maritorena, S., Siegel, D.A., 2005. Consistent merging of satellite ocean color data sets
1029 using a bio-optical model. *Remote Sensing of Environment* 94, 429-440.
- 1030 McGowan, J.A., Bograd, S.J., Lynn, R.J., Miller, A.J., 2003. The biological response to
1031 the 1977 regime shift in the California Current. *Deep-Sea Research Part II -*
1032 *Topical Studies in Oceanography* 50, 2567-2582.

- 1033 McPhaden, M.J., Zebiak, S.E., Glantz, M.H., 2006. ENSO as an integrating concept in
1034 Earth science. *Science* 314, 1740-1745.
- 1035 NOS 2008. CO-OPS specifications and deliverables for installation, operation, and
1036 removal of water level stations. Requirements and Developmental Division,
1037 Center for Operational Oceanographic Products and Services, National Ocean
1038 Service, NOAA.
- 1039 Peña, M.A., Bograd, S.J., 2007. Time series of the northeast Pacific. *Progress in*
1040 *Oceanography* 75, 115-119.
- 1041 Peterson, W.T., Schwing, F.B., 2003. A new climate regime in Northeast Pacific
1042 ecosystems. *Geophysical Research Letters* 30, 1896.
- 1043 Piatt, J.F., Harding, A.M.A., Shultz, M., Speckman, S.G., Van Pelt, T.I., Drew, G.S.,
1044 Kettle, A.B., 2007. Seabirds as indicators of marine food supplies: Cairns
1045 revisited. *Marine Ecology Progress Series* 352, 221-234.
- 1046 Ralston, S., Sakuma, K.M., Field, J.C., 2013. Interannual variation in pelagic juvenile
1047 rockfish (*Sebastes* spp.) abundance – going with the flow. *Fisheries*
1048 *Oceanography*, in press. doi:10.1111/fog.12022.
- 1049 Rice, J.C., Rochet, M.J., 2005. A framework for selecting a suite of indicators for
1050 fisheries management. *ICES Journal of Marine Science* 62, 516-527.
- 1051 Schwing, F.B., O'Farrell, M., Steger, J.M., Baltz, K., 1996. Coastal upwelling indices,
1052 west coast of North America, 1946-1995. NOAA-TM-NMFS-SWFSC-231.
- 1053 Schwing, F.B., Murphree, T., deWitt, L., Green, P.M., 2002. The evolution of oceanic
1054 and atmospheric anomalies in the northeast Pacific during the El Niño and La
1055 Niña events of 1995-2001. *Progress in Oceanography* 54, 459-491.
- 1056 Schwing, F.B., Bond, N.A., Bograd, S.J., Mitchell, T., Alexander, M.A., Mantua, N.,
1057 2006. Delayed coastal upwelling along the US West Coast in 2005: A historical
1058 perspective. *Geophysical Research Letters* 33, L22S01.
- 1059 Sydeman, W.J., Thompson, S.A., 2010. The California Current Integrated Ecosystem
1060 Assessment (IEA), Module II: Trends and variability in climate-ecosystem state.
1061 Report to NOAA, SWFSC, Environmental Research Division. Pacific Grove,
1062 California.
- 1063 Sydeman, W.J., Hester, M., Thayer, J.A., Gress, F., Martin, P., Buffa, J., 2001. Climate
1064 change, reproductive performance and diet composition of marine birds in the
1065 southern California Current System, 1967-1997. *Progress in Oceanography* 49,
1066 309-329.
- 1067 Sydeman, W.J., Bradley, R.W., Warzybok, P., Abraham, C.L., Jahncke, J., Hyrenbach,
1068 K.D., Kousky, V., Hipfner, J.M., Ohman, M.D., 2006. Planktivorous auklet
1069 *Ptychoramphus aleuticus* responses to ocean climate, 2005: Unusual
1070 atmospheric blocking? *Geophysical Research Letters* 33, L22S09.
- 1071 Sydeman, W.J., Mills, K.L., Santora, J.A., Thompson, S.A., Bertram, D.F., Morgan,
1072 K.H., Wells, B.K., Hipfner, J.M., Wolf, S.G., 2009. Seabirds and climate in the
1073 California Current--A synthesis of change. *California Cooperative Oceanic*
1074 *Fisheries Investigations Reports* 50, 82-104.
- 1075 Sydeman, W.J., Santora, J.A., Thompson, S.A., Marinovic, B., Di Lorenzo, E., 2013.
1076 Increasing variance in North Pacific climate explains unprecedented ecosystem
1077 variability off California. *Global Change Biology*, in press.

- 1078 Thompson, S.A., Sydeman, W.J., Santora, J.A., Black, B.A., Suryan, R.M.,
1079 Calambokidis, J., Peterson, W.T., Bograd, S.J., 2012. Linking predators to
1080 seasonality of upwelling: Using food web indicators and path analysis to infer
1081 trophic connections. *Progress in Oceanography* 101, 106-120.
- 1082 Wilkerson, F.P., Lassiter, A.M., Dugdale, R.C., Marchi, A., Hogue, V.E., 2006. The
1083 phytoplankton bloom response to wind events and upwelled nutrients during the
1084 CoOP WEST study. *Deep-Sea Research Part II* 53, 3023-3048.
- 1085 Wolter, K., Timlin, M.S., 1993. Monitoring ENSO in COADS with a seasonally adjusted
1086 principal component index. In *Proceedings of the 17th Climate Diagnostics
1087 Workshop*, Norman, Oklahoma, pp. 52-57.
- 1088 Zhang, Y., Wallace, J.M., Battisti, D.S., 1997. ENSO-like interdecadal variability: 1900-
1089 93. *Journal of Climate* 10, 1004-1020.
- 1090

1091

1092 Table 1. Data sets used. Shown for each variable is the year of the beginning of the
 1093 full time series (all data sets extend through 2010) and the source for the data.
 1094

Variable Type	Variable	Beginning Year of Time Series	Data Source
Sub-tropical Climate Indices	Southern Oscillation Index	1900	Climate Analysis Section, National Center for Atmospheric Research
	Multivariate ENSO Index	1950	Earth System Research Laboratory, NOAA
	Oceanic Nino Index	1950	Center for Climate Prediction, National Weather Service, NOAA
Sub-arctic Climate Indices	North Pacific Index	1900	Climate Analysis Section, National Center for Atmospheric Research
	North Pacific Gyre Oscillation	1950	Emanuele Di Lorenzo, Georgia Institute of Technology
	Pacific Decadal Oscillation	1900	Joint Institute for the Study of the Atmosphere and Ocean, University of Washington
Upwelling	Northern Oscillation Index	1970	Pacific Fisheries Environmental Laboratory, NOAA
	Bakun Upwelling Index 36°N	1946	Environmental Research Division, NOAA
	Bakun Upwelling Index 39°N	1946	Environmental Research Division, NOAA
California Current Flow	California Current	2002	Howard Freeland, Fisheries and Oceans Canada
	Point Reyes Cell 0	2001	Bodega Marine Lab, University of California Davis
	Point Reyes Cell 1	2001	
	Point Reyes Cell 2	2001	
	Point Reyes Cell 3	2001	
Wind Stress	Bodega Bay	1982	Marisol Garcia-Reyes, University of California Davis
	San Francisco	1982	
	Half Moon Bay	1982	
	Monterey Bay	1982	
Sea Level	South Beach	1967	National Water Level Observation Network, Center for Operational Oceanographic Products and Services
	Crescent City	1933	
	San Francisco	1901	
Sea Surface Temperature	Point Arena	1982	NOAA
	Bodega Marine Lab	1988	Bodega Ocean Observing Node, Bodega Marine Lab, University of California Davis
	Bodega Bay	1981	NOAA
	San Francisco	1983	
	Farallon Islands	1955	Scripps Institution of Oceanography Shore Stations Program
	Half Moon Bay	1981	NOAA
Monterey Bay	1987		

Salinity	Bodega Marine Lab	1988	Bodega Ocean Observing Node, Bodega Marine Lab, University of California Davis
	Farallon Islands	1955	Scripps Institution of Oceanography Shore Stations Program
Air Temperature	Fort Ross	1950	National Climate Data Center, NOAA Bodega Ocean Observing Node, Bodega Marine Lab, University of California Davis
	Bodega Marine Lab	1988	
	San Francisco Pacifica	1959 1984	National Climate Data Center, NOAA
	Half Moon Bay	1939	
Precipitation	Fort Ross	1931	National Climate Data Center, NOAA
	San Francisco Pacifica	1959 1984	
	Half Moon Bay	1939	
Biological	Chlorophyll-a Concentration	1997	Mati Kahru, Scripps Photobiology Group, Scripps Institution of Oceanography
	Seabird Reproductive Success	1971, 1972	PRBO Conservation Science

1096
 1097 Table 2. Trends based on Spearman rank correlation for physical variables from 1990
 1098 to 2010 (n=252), except for current flow which spans 2002 to 2010 (n=108). Shading
 1099 indicates significance (p<0.05) without adjustment for autocorrelation. Climate indices,
 1100 the Northern Oscillation Index, California Current flow, and variable type first principal
 1101 components (PC1s) were subjected to quadratic regression to test for non-linearity in
 1102 patterns of change (*denotes variables with significant quadratic terms).
 1103

		Spearman rho	p-value
Sub-tropical Climate Indices	Southern Oscillation Index*	-0.31	<0.0001
	Multivariate ENSO Index*	-0.31	<0.0001
	Oceanic Nino Index*	-0.20	0.0017
Sub-arctic Climate Indices	North Pacific Index	0.05	0.4571
	North Pacific Gyre Oscillation*	0.52	<0.0001
	Pacific Decadal Oscillation*	-0.25	0.0001
Upwelling	Northern Oscillation Index*	0.27	<0.0001
	Bakun Upwelling Index 36°N	0.11	0.0813
	Bakun Upwelling Index 39°N	0.17	0.0084
	Bakun Upwelling Index PC1*	0.16	0.0132
California Current Flow	California Current	0.14	0.1639
	Point Reyes Cell 0	0.08	0.4329
	Point Reyes Cell 1	0.12	0.2239
	Point Reyes Cell 2	0.19	0.0436
	Point Reyes Cell 3	0.08	0.4395
	Point Reyes Flow PC1	0.12	0.2070
Wind Stress	Bodega Bay	0.13	0.0331
	San Francisco	0.20	0.0014
	Half Moon Bay	0.18	0.0046
	Monterey Bay	0.15	0.0185
	Wind Stress PC1*	0.18	0.0051
Sea Level	South Beach	0.03	0.6420
	Crescent City	-0.27	<0.0001
	San Francisco	0.00	0.9947
	Sea Level PC1	-0.09	0.1578
Sea Surface Temperature	Point Arena	-0.24	0.0002
	Bodega Marine Lab	-0.08	0.1961
	Bodega Bay	-0.17	0.0060
	San Francisco	-0.09	0.1495
	Farallon Islands	-0.20	0.0011
	Half Moon Bay	-0.17	0.0071
	Monterey Bay	0.02	0.7585
	SST PC1*	-0.17	0.0061
Salinity	Bodega Marine Lab	0.08	0.1885
	Farallon Islands	0.01	0.8509
	Salinity PC1*	0.08	0.1936
Air Temperature	Fort Ross	-0.03	0.6805
	Bodega Marine Lab	-0.35	<0.0001
	San Francisco	-0.20	0.0012
	Pacifica	0.17	0.0075
	Half Moon Bay	-0.07	0.2865
	Air Temperature PC1*	-0.15	0.0154

Precipitation	Fort Ross	0.06	0.3673
	San Francisco	0.04	0.4828
	Pacifica	0.01	0.9201
	Half Moon Bay	0.00	0.9986
	Precipitation PC1	0.02	0.7403

1104
1105

1106
 1107 Table 3. Results of principal components analysis within variable types, 1990-2010 (Pt.
 1108 Reyes surface flow, 2002-2010). A. Eigenvalues and variance explained by the first two
 1109 principal components. B. Site loadings within variable type.
 1110
 1111

A.

	Component	Eigenvalue	Proportion	Cumulative
Bakun Upwelling	1	1.701	0.850	0.850
	2	0.299	0.150	1.000
Surface Flow, Pt. Reyes	1	3.349	0.837	0.837
	2	0.467	0.117	0.954
Wind Stress	1	3.287	0.822	0.822
	2	0.405	0.101	0.923
Sea level	1	2.545	0.848	0.848
	2	0.309	0.103	0.951
Sea Surface Temperature	1	4.989	0.713	0.713
	2	0.559	0.080	0.793
Salinity	1	1.734	0.867	0.867
	2	0.266	0.133	1.000
Air Temperature	1	3.235	0.647	0.647
	2	0.723	0.153	0.800
Precipitation	1	3.660	0.915	0.915
	2	0.157	0.039	0.954

1112
 1113
 1114

B.

	Site	Eigenvector Loadings	
		1	2
Bakun Upwelling	36°N	0.707	0.707
	39°N	0.707	-0.707
Surface Flow, Pt. Reyes	Cell 0	0.478	0.626
	Cell 1	0.514	0.334
	Cell 2	0.523	-0.321
	Cell 3	0.484	-0.627
Wind Stress	Bodega Bay	0.513	0.016
	San Francisco	0.465	0.815
	Half Moon Bay	0.514	-0.344
	Monterey Bay	0.507	-0.462
Sea level	South Beach	0.573	-0.642
	Crescent City	0.596	-0.101
	San Francisco	0.563	0.760
Sea Surface Temperature	Point Arena	0.356	-0.628
	Bodega Marine Lab	0.399	-0.176
	Bodega Bay	0.387	0.124
	San Francisco	0.404	0.065
	Farallon Islands	0.407	-0.138
	Half Moon Bay	0.347	0.729
	Monterey Bay	0.338	0.068
Salinity	Farallon Islands	0.707	0.707
	Bodega Marine Lab	0.707	-0.707
Air Temperature	Fort Ross	0.478	-0.005
	Bodega Marine Lab	0.401	-0.620
	San Francisco	0.490	0.018

	Pacifica	0.368	0.779
	Half Moon Bay	0.485	-0.092
Precipitation	Fort Ross	0.491	0.857
	San Francisco	0.499	-0.142
	Pacifica	0.507	-0.297
	Half Moon Bay	0.503	-0.396

1115

Table 4. Interrelationships between environmental indicators. Spearman rank cross-correlations (Spearman rho) for monthly anomalies of climate indicators and first principal components of ocean indicators based on monthly anomalies, 1990-2010 (n=252) or current flow (2002-2010, n=108). Shading indicates rho > |0.5|.

	Multivariate ENSO Index	Southern Oscillation Index	Oceanic Nino Index	North Pacific Index	North Pacific Gyre Oscillation	Pacific Decadal Oscillation	Northern Oscillation Index
Southern Oscillation Index	0.76						
Oceanic Nino Index	0.93	0.74					
North Pacific Index	-0.28	-0.27	-0.30				
North Pacific Gyre Oscillation	-0.40	-0.33	-0.32	-0.04			
Pacific Decadal Oscillation	0.51	0.39	0.46	-0.34	-0.40		
Northern Oscillation Index	-0.51	-0.50	-0.48	0.44	0.25	-0.40	
Upwelling Index PC1	-0.26	-0.12	-0.23	0.33	0.19	-0.34	0.60
California Current Flow	-0.40	-0.38	-0.43	0.09	0.30	-0.43	0.33
Surface Flow, Pt. Reyes PC1	-0.22	-0.15	-0.24	0.10	0.02	-0.10	0.54
Wind Stress PC1	-0.18	-0.11	-0.16	0.25	0.18	-0.24	0.61
Sea Level PC1	0.46	0.31	0.42	-0.38	-0.29	0.50	-0.76
Sea Surface Temperature PC1	0.43	0.30	0.37	-0.33	-0.38	0.59	-0.60
Salinity PC1	-0.20	-0.08	-0.15	0.20	0.31	-0.48	0.38
Air Temperature PC1	0.25	0.24	0.21	-0.32	-0.23	0.51	-0.45
Precipitation PC1	0.01	-0.04	-0.01	-0.12	0.00	0.10	-0.37

	Upwelling Index PC1	California Current Flow	Surface Flow, Pt. Reyes PC1	Wind Stress PC1	Sea Level PC1	Sea Surface Temperature PC1	Salinity PC1	Air Temperature PC1
California Current Flow	0.22							
Surface Flow, Pt. Reyes PC1	0.33	0.10						
Wind Stress PC1	0.66	0.18	0.59					
Sea Level PC1	-0.66	-0.39	-0.43	-0.55				
Sea Surface Temperature PC1	-0.57	-0.39	-0.40	-0.54	0.70			
Salinity PC1	0.37	0.40	0.12	0.38	-0.62	-0.57		
Air Temperature PC1	-0.41	-0.24	-0.06	-0.34	0.44	0.69	-0.39	
Precipitation PC1	-0.41	-0.12	-0.33	-0.47	0.50	0.18	-0.28	0.04

Table 5. Seasonal multivariate ocean-climate indicators (MOCI) derived by principal component analysis (PCA) on detrended physical variables within each season, 1990-2010. A. Eigenvalues and proportion explained for the first and second principal components. B. Eigenvector loadings for first and second principal components by season. Shading indicates values $> |0.2|$.

A.

Season	Component	Eigenvalue	Proportion	Cumulative
Winter	1	18.943	0.557	0.557
	2	5.000	0.147	0.704
Spring	1	18.163	0.534	0.534
	2	4.628	0.136	0.670
Summer	1	13.025	0.383	0.383
	2	4.673	0.138	0.521
Fall	1	13.729	0.404	0.404
	2	4.084	0.120	0.524

B.

		Winter		Spring		Summer		Fall	
		1	2	1	2	1	2	1	2
Sub-tropical Climate Indices	Southern Oscillation Index	0.149	0.113	0.063	0.248	0.111	-0.200	0.148	0.305
	Multivariate ENSO Index	0.164	0.087	0.151	0.151	0.193	-0.132	0.147	0.330
	Oceanic Nino Index	0.161	0.120	0.125	0.191	0.176	-0.195	0.135	0.364
Sub-arctic Climate Indices	North Pacific Index	-0.145	0.014	-0.078	-0.206	-0.182	0.199	-0.090	-0.091
	North Pacific Gyre Oscillation	-0.073	-0.162	-0.147	-0.097	-0.071	-0.129	-0.102	0.036
	Pacific Decadal Oscillation	0.157	0.206	0.182	0.028	0.196	0.031	0.219	0.012
Upwelling	Northern Oscillation Index	-0.218	0.046	-0.191	-0.122	-0.164	0.185	-0.207	-0.262
	Bakun Upwelling Index 36°N	-0.174	0.017	-0.192	-0.002	-0.136	-0.057	-0.122	-0.068
	Bakun Upwelling Index 39°N	-0.193	0.111	-0.211	-0.008	-0.189	0.081	-0.110	0.074
Wind Stress	Bodega Bay	-0.193	0.119	-0.180	0.083	-0.076	0.265	-0.196	0.195
	San Francisco	-0.193	0.147	-0.191	0.106	-0.027	0.152	-0.199	0.181
	Half Moon Bay	-0.190	0.139	-0.141	0.011	0.052	0.218	-0.187	0.151
	Monterey Bay	-0.177	0.137	-0.191	0.071	0.007	0.225	-0.204	0.081
Sea Level	South Beach	0.200	-0.142	0.199	0.001	0.251	-0.008	0.169	0.224
	Crescent City	0.219	-0.086	0.222	0.017	0.235	0.039	0.212	0.172
	San Francisco	0.213	-0.089	0.202	-0.102	0.179	0.203	0.225	0.224
Sea Surface Temperature	Point Arena	0.192	0.057	0.184	0.048	0.236	-0.070	0.198	-0.042
	Bodega Marine Lab	0.204	0.129	0.209	0.037	0.210	0.070	0.220	-0.034
	Bodega Bay	0.196	0.165	0.222	-0.034	0.173	0.213	0.194	-0.159
	San Francisco	0.188	0.157	0.211	0.087	0.242	0.141	0.219	-0.106
	Farallon Islands	0.215	0.092	0.204	0.024	0.240	0.092	0.218	-0.019
	Half Moon Bay	0.148	0.166	0.168	0.065	0.184	0.233	0.171	-0.211
Salinity	Monterey Bay	0.171	0.187	0.184	-0.055	0.205	0.098	0.144	0.004
	Bodega Marine Lab	-0.170	0.125	-0.169	0.138	-0.158	-0.038	-0.129	0.164
Farallon Islands		-0.138	0.059	-0.183	0.179	-0.124	-0.261	-0.103	0.200
	Fort Ross	0.169	0.169	0.162	0.191	0.199	0.059	0.157	-0.121
Air Temperature	Bodega Marine Lab	0.151	0.178	0.172	0.151	0.094	0.115	0.197	-0.180
	San Francisco	0.150	0.169	0.184	0.169	0.226	0.057	0.167	-0.205
	Pacifica	0.086	0.316	0.024	0.371	0.213	-0.006	0.099	-0.209
	Half Moon Bay	0.179	0.149	0.189	0.138	0.224	-0.029	0.190	-0.076
	Fort Ross	0.138	-0.287	0.166	-0.244	0.131	-0.207	0.118	0.144
Precipitation	San Francisco	0.144	-0.315	0.087	-0.359	0.133	-0.271	0.130	0.138
	Pacifica	0.129	-0.338	0.122	-0.358	0.092	-0.330	0.155	0.115
	Half Moon Bay	0.129	-0.323	0.108	-0.381	0.055	-0.327	0.180	0.066

Table 6. Cross-correlation of seasonal MOCI produced by principal component analysis (PCA), local variables only combined with PCA, and climate indices only combined with PCA. In each cell, Spearman rho is the top value and the p-value is below. Shading indicates significance ($p < 0.05$). Winter, spring, and summer $n = 21$; fall $n = 20$.

	Fall _{x-1}		Winter		Spring		Summer	
	MOCI	Local Variables	MOCI	Local Variables	MOCI	Local Variables	MOCI	Local Variables
Local Variables	0.97 <0.0001		0.98 <0.0001		0.99 <0.0001		0.97 <0.0001	
Climate Indices	0.71 0.0001	0.65 0.0018	0.78 <0.0001	0.73 0.0002	0.73 0.0002	0.67 0.0009	0.53 0.0130	0.43 0.0542

Table 7. Spearman rank correlations of seabird reproductive success residuals and $PC1_{\text{seabirds}}$ and seasonal MOCI. In each cell are Spearman rho and p-value. $N = 18$ for all relationships. Shading indicates relationships where $p < 0.05$.

	MOCI1- Winter	MOCI2- Winter	MOCI1- Spring	MOCI2- Spring	MOCI1- Summer	MOCI2- Summer	MOCI1- Fall	MOCI2- Fall
Common Murre	-0.59 0.01	-0.10 0.70	-0.73 <0.01	0.04 0.87	0.01 0.98	-0.57 0.01	-0.31 0.21	0.15 0.55
Pigeon Guillemot	-0.35 0.16	-0.03 0.92	-0.62 0.01	0.25 0.32	-0.13 0.60	-0.59 0.01	0.16 0.53	0.27 0.28
Cassin's Auklet	-0.19 0.45	-0.09 0.73	-0.48 0.04	-0.06 0.82	-0.50 0.03	-0.38 0.12	-0.17 0.51	0.29 0.24
Brandt's Cormorant	-0.33 0.18	-0.13 0.60	-0.61 0.01	-0.22 0.38	-0.39 0.11	-0.66 <0.01	-0.21 0.40	0.16 0.53
$PC1_{\text{seabirds}}$	-0.48 0.04	-0.13 0.62	-0.79 <0.01	0.01 0.96	-0.44 0.07	-0.68 <0.01	-0.15 0.55	0.28 0.26

Figure 1. Indicators of El Niño/La Niña, transport from the tropics. A. Southern Oscillation Index (SOI, sign reversed), B. Multivariate ENSO Index (MEI), and C. Oceanic Niño Index (ONI), 1990-2010. Blue line indicates LOESS smoothing function with sampling proportion of 0.2. Dashed lines show ± 1 long-term standard deviation based on varying time series (SOI: 1900-2010, MEI and ONI: 1950-2010).

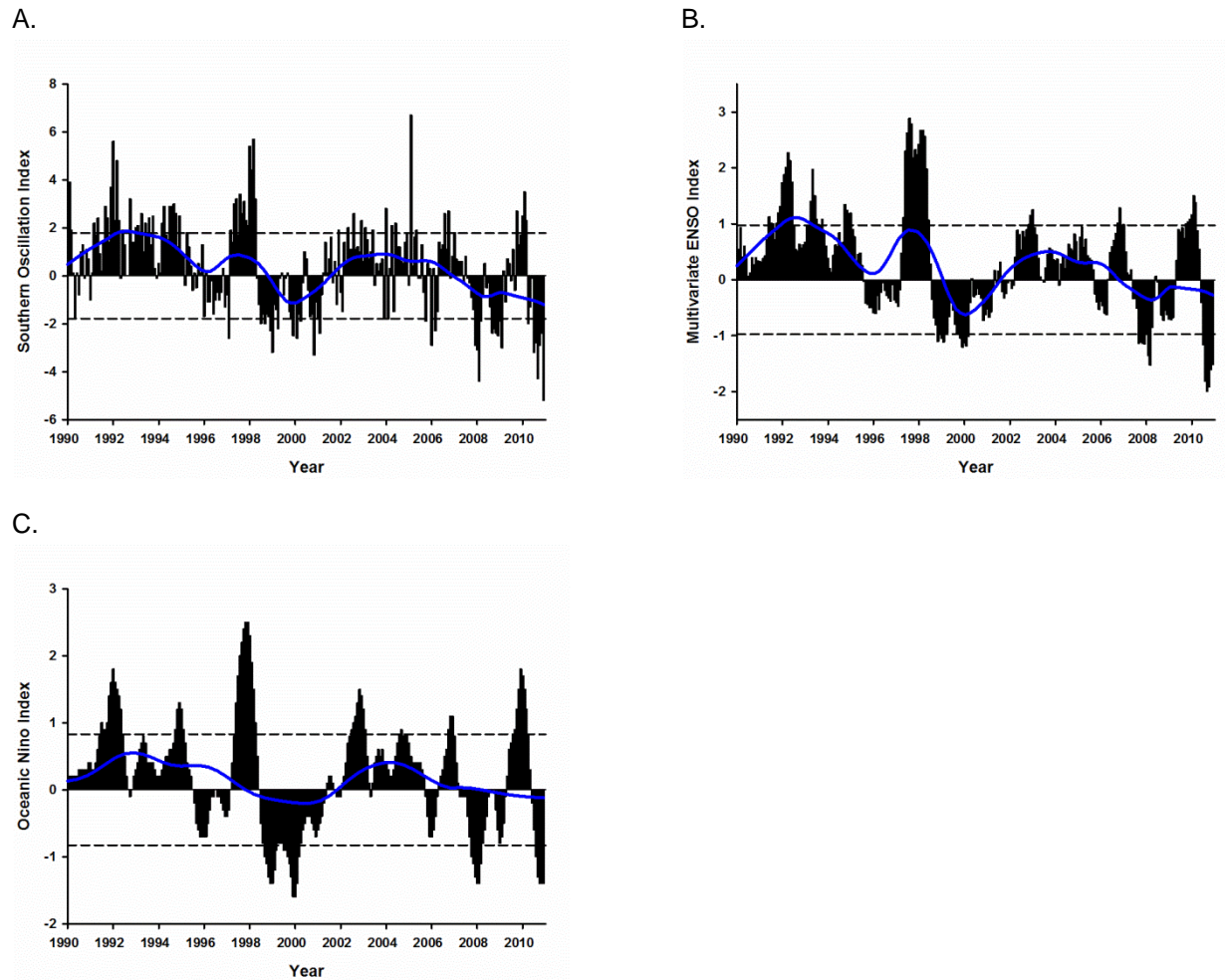
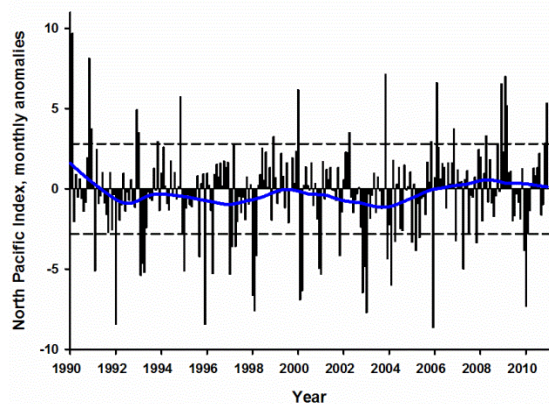
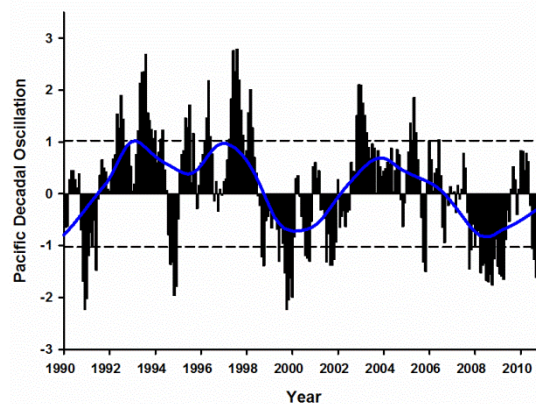


Figure 2. Indicators of transport from the sub-arctic North Pacific. A. North Pacific Index (NPI) monthly anomalies, B. Pacific Decadal Oscillation (PDO), and C. North Pacific Gyre Oscillation Index (NPGO), 1990-2010. Blue line indicates LOESS smoothing function with sampling proportion of 0.2. Dashed lines show ± 1 long-term standard deviation based on varying time series (NPI and PDO: 1900-2010 and NPGO: 1950-2010).

A.



B.



C.

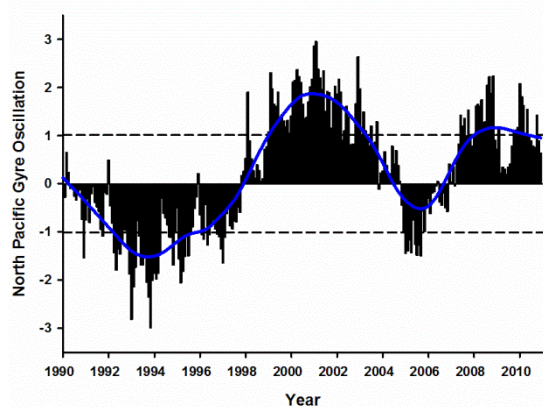
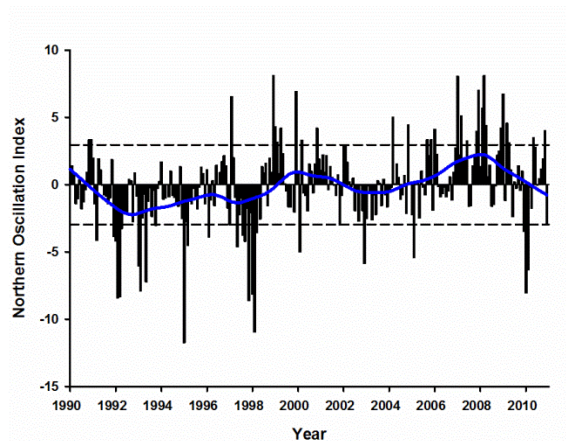


Figure 3. A. Indicators of regional upwelling. Northern Oscillation Index (NOI) and B. the first principal component (PC1) of Bakun Upwelling Index at 36°N and 39°N, 1990-2010. Blue line indicates LOESS smoothing function with sampling proportion of 0.2. Dashed lines show ± 1 long-term standard deviation for NOI (1970-2010) and 1990-2010 standard deviation for Upwelling PC1.

A.



B.

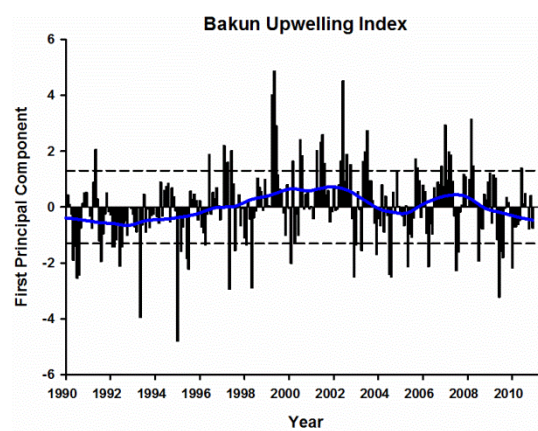


Figure 4. Indicators of large-scale and local current flow. A. California Current flow measured by Argo and B. surface flow at Pt. Reyes, first principal component of all cells, 2002-2010. Blue line indicates LOESS smoothing function with sampling proportion of 0.2. Dashed lines show ± 1 standard deviation.

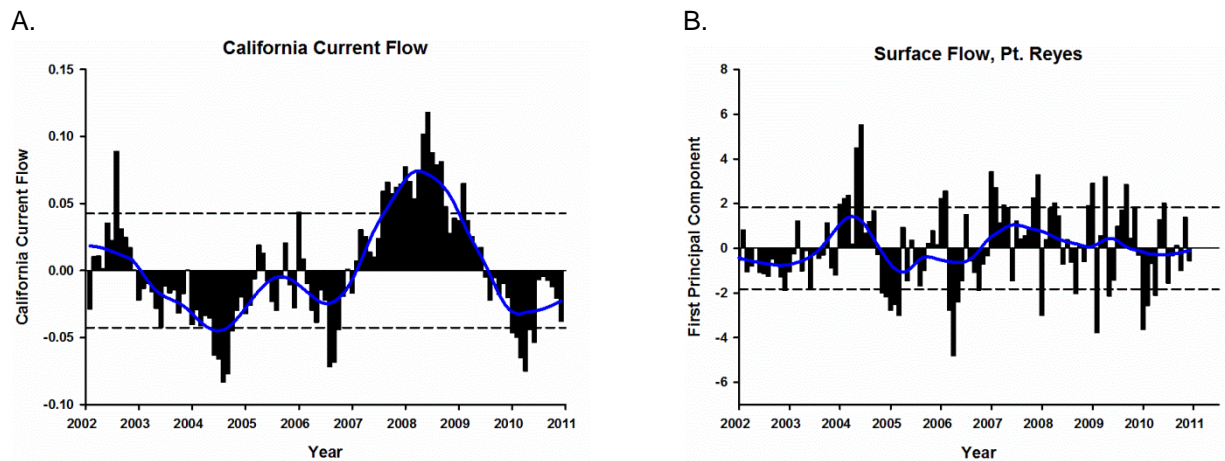


Figure 5. Indicators of regional coupled wind and hydrography (1990-2010): A. wind stress, B. sea surface temperature, C. sea level, and D. salinity. Blue line indicates LOESS smoothing function with sampling proportion of 0.2. Dashed lines show ± 1 standard deviation.

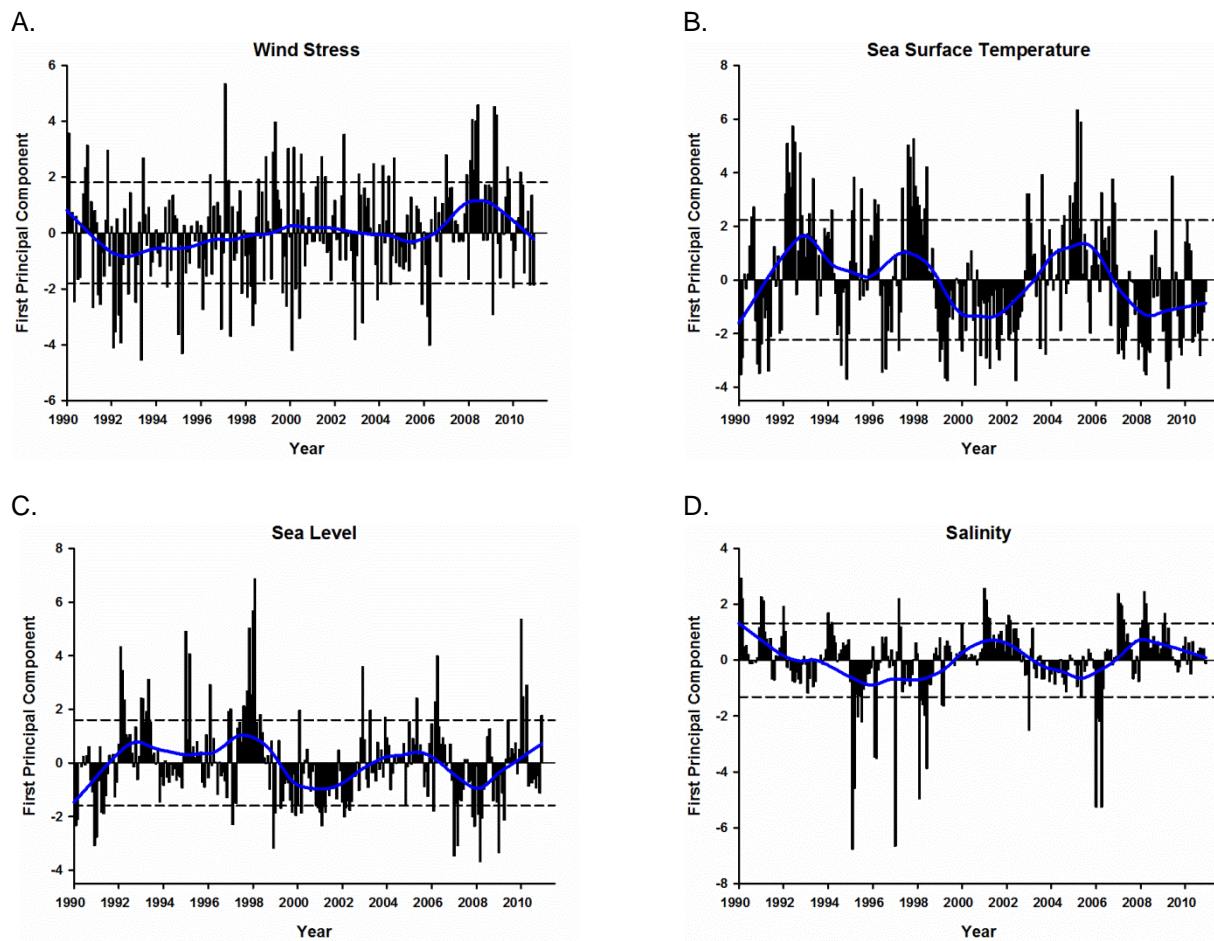


Figure 6. Indicators of regional atmospheric conditions. First principal components of A. air temperature and B. precipitation, 1990-2010. Blue line indicates LOESS smoothing function with sampling proportion of 0.2. Dashed lines show ± 1 standard deviation.

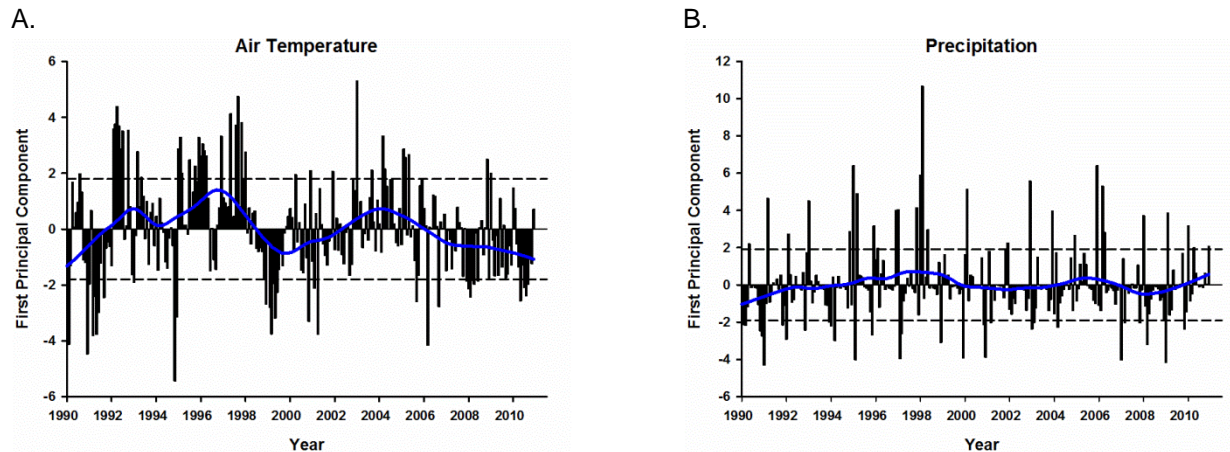


Figure 7. The first principal component variable loadings plotted against the second principal component variable loadings (PC space), 1990-2010 for seasonal MOCI. MOCI were calculated from residuals of seasonal averages. A. winter, B. spring, C. summer, and D. fall. Labels for circular symbols indicate climate variables. SOI: Southern Oscillation Index; MEI: Multivariate ENSO Index; NOI: Northern Oscillation Index; NPGO: North Pacific Gyre Oscillation; NPI: North Pacific Index; ONI: Oceanic Nino Index; PDO: Pacific Decadal Oscillation. ☆: sea level; ■: sea surface temperature (SST); x: salinity; ▼: Bakun Upwelling Index; : wind stress; ▲: air temperature; ◆: precipitation.

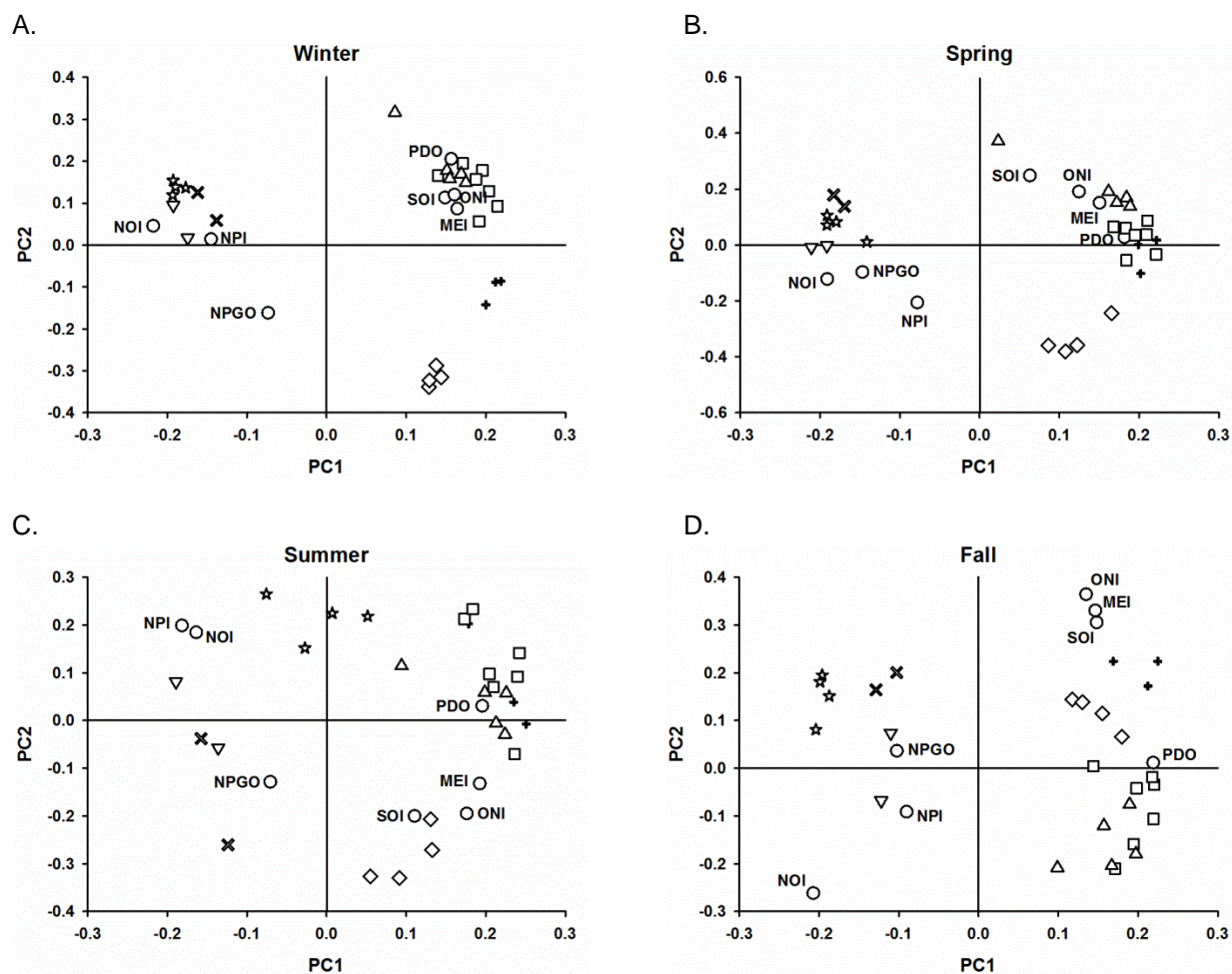


Figure 8. Seasonal MOCI against time for A. winter, B. spring, C. summer and D. fall, 1990-2010. MOCI were calculated from residuals of seasonal averages. Blue line shows LOESS smoothing function with sampling proportion = 0.3. Dashed lines show ± 1 standard deviation.

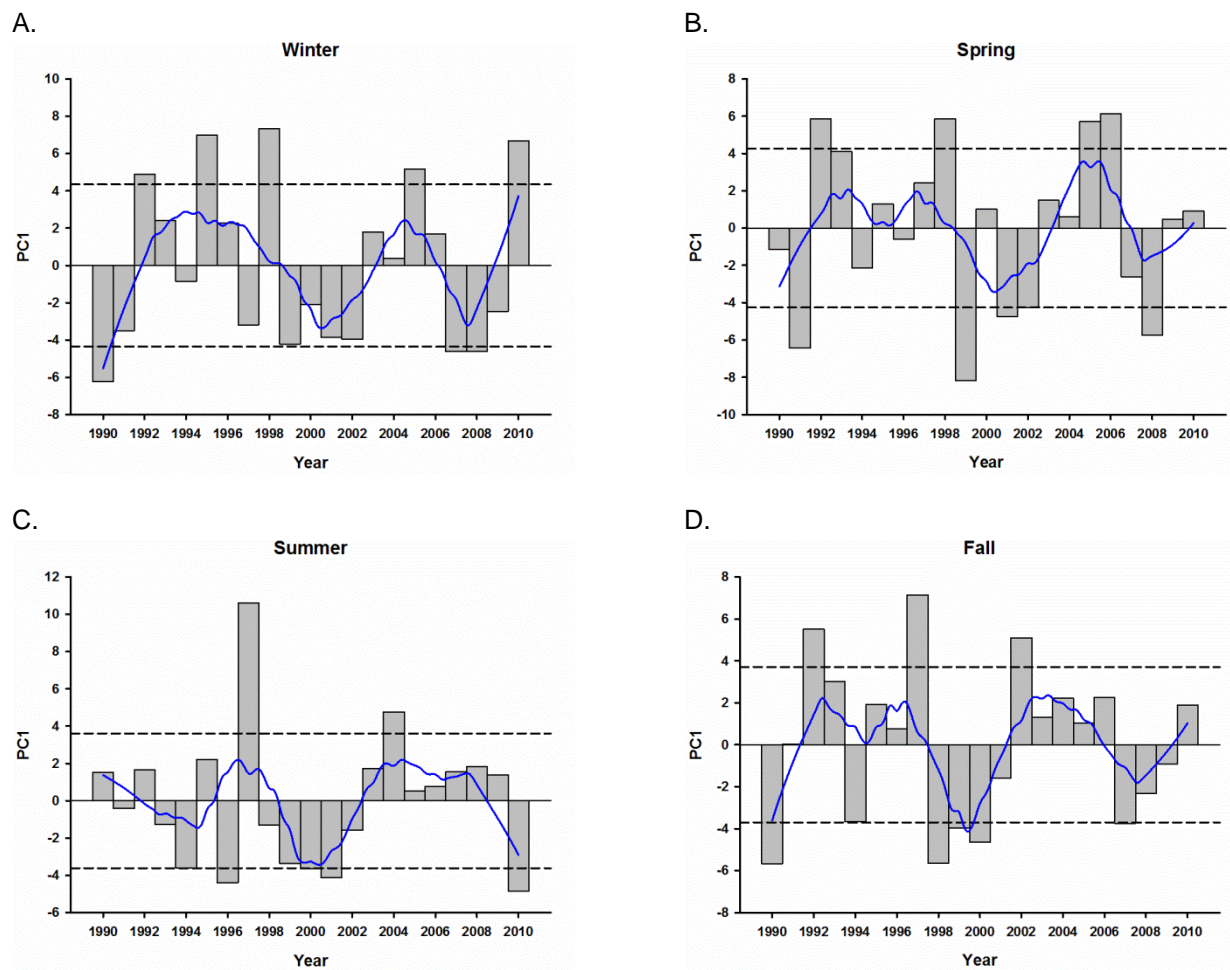


Figure 9. Seasonal MOCI time series, 1990-2010. Smoothed line is based on LOESS with sampling proportion of 0.3. Dashed lines are 1 s.d. for the time series. 1 standard deviation was also calculated for each season. Red points indicate values greater than 1 seasonal s.d. and blue points indicate values less than 1 seasonal s.d.

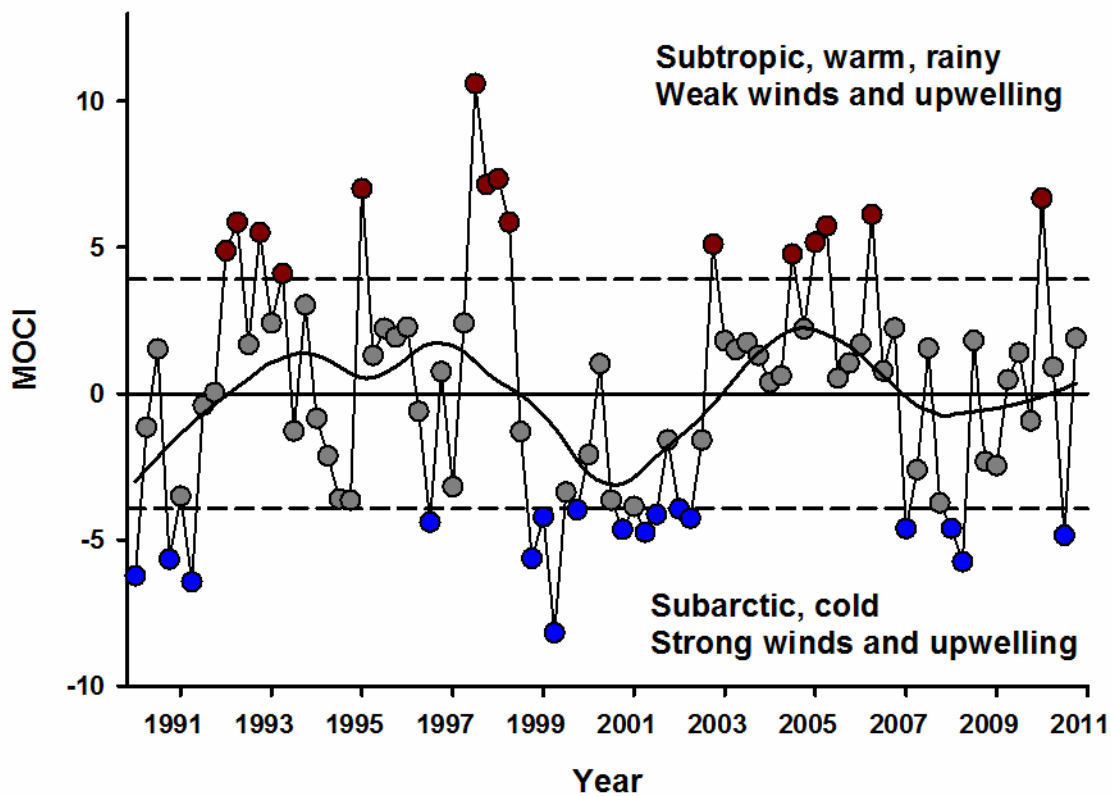
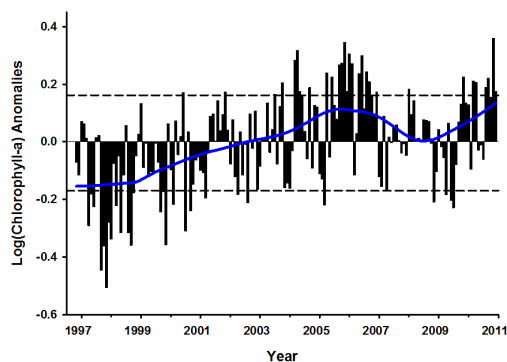
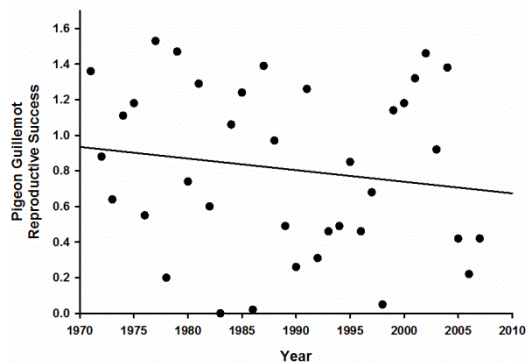


Figure 10. A. Log chlorophyll-a abundance anomalies (1997-2011). Blue line indicates LOESS smoothing function with sampling proportion of 0.3. Dashed lines show ± 1 standard deviation. Seabird reproductive success with linear regression for B. pigeon guillemot (1971-2007), C. Cassin's auklet (1971-2007), D. common murre (1972-2007), and E. Brandt's cormorant (1971-2007). F. Seabird first principal component, 1972-2007.

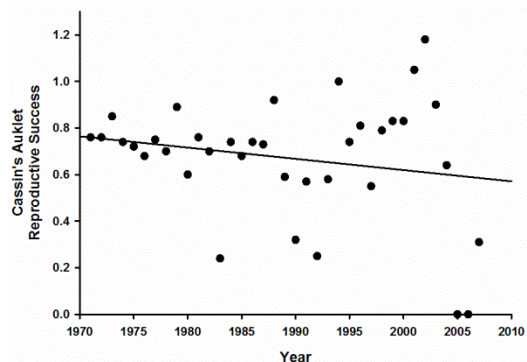
A.



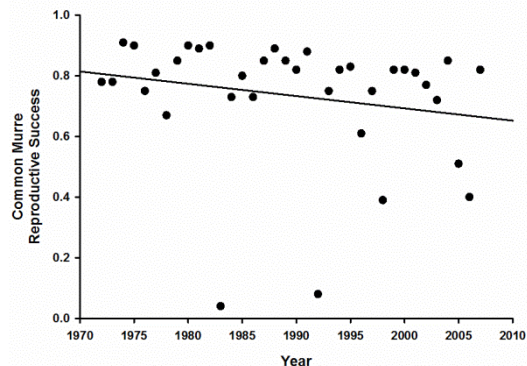
B.



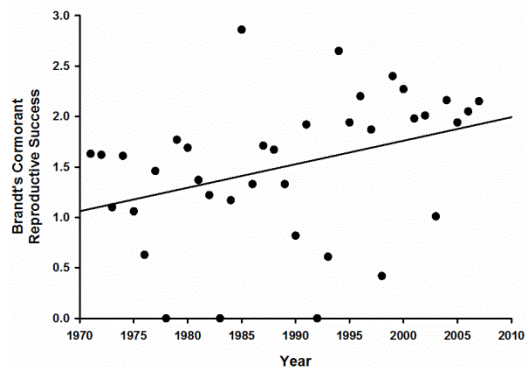
C.



D.



E.



F.

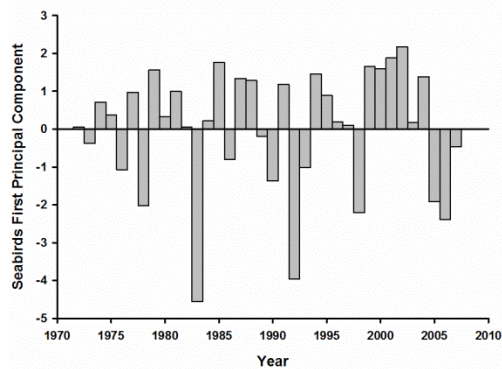
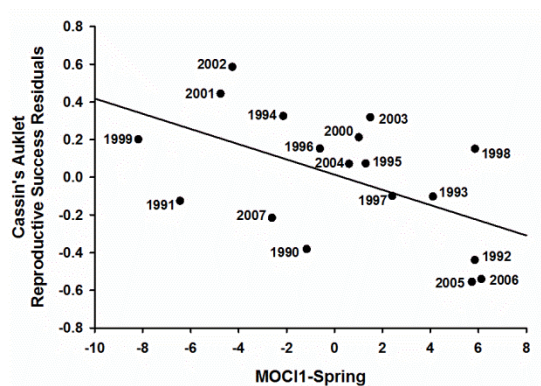
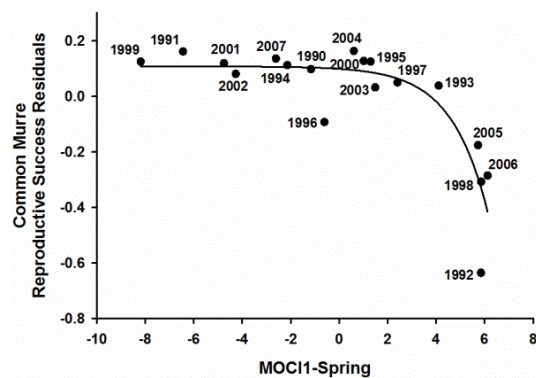


Figure 11. Significant relationships for spring MOCI (PC1) and residuals of reproductive success for A. Cassin's auklet, B. common murre, C. pigeon guillemot, and D. Brandt's Cormorant. E. Relationship of MOCI1-spring and a $PC1_{\text{seabirds}}$. Regression lines are linear with the exception of common murre, which is an exponential curve.

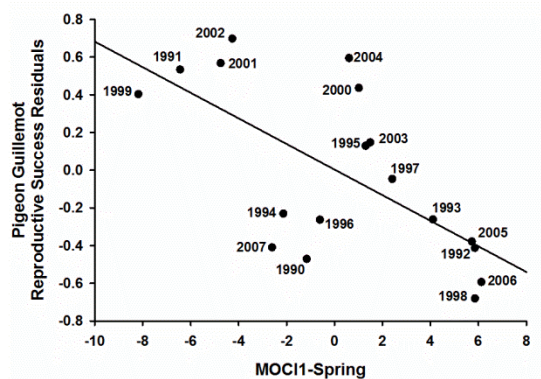
A.



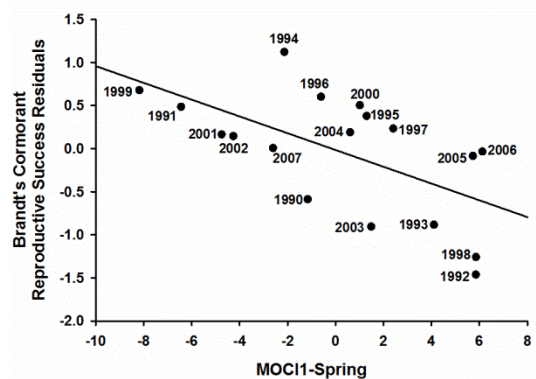
B.



C.



D.



E.

